AD_____
blank)

Award Number: W81XWH-10-1-0523

TITLE: Early Detection of Ovarian Cancer by Contrast-Enhanced Ultrasound-Targeted Imaging

PRINCIPAL INVESTIGATOR: Animesh Barua, Ph.D.

CONTRACTING ORGANIZATION: Rush University Medical Center
Chicago, IL 60612

REPORT DATE: July 2012

TYPE OF REPORT: Annual

PREPARED FOR: U.S. Army Medical Research and Materiel Command
Fort Detrick, Maryland 21702-5012

DISTRIBUTION STATEMENT: Approved for Public Release;
Distribution Unlimited

REPORT DOCUMENTATION PAGE

Form Approved
OMB No. 0704-0188

1. REPORT DATE	2. REPORT TYPE	3. DATES COVERED
July 2012	Annual	1 July, 2011 ï 30 June, 2012

4. TITLE AND SUBTITLE

Early Detection of Ovarian Cancer by Contrast-Enhanced Ultrasound-Targeted Imaging

5a. CONTRACT NUMBER

5b. GRANT NUMBER
W81XWH-10-1-0523

5c. PROGRAM ELEMENT NUMBER

5d. PROJECT NUMBER

5e. TASK NUMBER

5f. WORK UNIT NUMBER

Animesh Barua, Ph.D.

E-Mail: Animesh_Barua@rush.edu

7. PERFORMING ORGANIZATION NAME(S) AND ADDRESS(ES)

Rush University Medical Center,
Chicago, IL 60612

8. PERFORMING ORGANIZATION REPORT NUMBER

9. SPONSORING / MONITORING AGENCY NAME(S) AND ADDRESS(ES)
U.S. Army Medical Research and Materiel Command
Fort Detrick Maryland 21702-5012

10. SPONSOR/MONITOR'S ACRONYM(S)

11. SPONSOR/MONITOR'S REPORT NUMBER(S)

12. DISTRIBUTION / AVAILABILITY STATEMENT
Approved for Public Release; Distribution Unlimited

13. SUPPLEMENTARY NOTES

14. ABSTRACT

Due to the lack of an early detection test, most cases of OVCA are detected at late stages when the 5-year survival rate is <10%. Transvaginal ultrasound (TVUS) imaging, the currently favored method, it cannot detect OVCA at early stage due to its limited resolution. Tumor related malignant nuclear transformation occurs early in tumor development and leads to the release of Nuclear Matrix Proteins (NMP) into the circulation. Tumor associated neoangiogenesis (TAN) follows malignant nuclear transformation.$\alpha_v\beta_3$-integrins and death receptors (DR) 6 are two markers of ovarian TAN expressed by neoangiogenic microvessels. DR6 is also secreted in serum. If the detection limit of TVUS imaging can be enhanced, $\alpha_v\beta_3$-integrins expressing microvessels can be an *in vivo* imaging marker of ovarian TAN and may be used together with serum anti-NMP antibodies and DR6 to detect early stage OVCA. Our overall goal is to improve the TVUS detectability of ovarian TAN vessels at early stage by $\alpha_v\beta_3$-integrins targeted contrast enhanced ultrasound (CE-US) molecular imaging. This goal is being achieved by 3 specific aims. The results of aim 1 and aim 2 suggest that CE-US molecular imaging targeting ovarian $\alpha_v\beta_3$-integrins can detect ovarian TAN at early stage OVCA in the laying hen model of spontaneous OVCA. Changes in OVCA related CE-US imaging indices are associated with the elevation of serum DR6 levels. Serum prevalence of anti-NMP antibodies is associated with malignant nuclear transformation and can be detected from serum even before the tumor becomes detectable through TVUS imaging.

15. SUBJECT TERMS

Ovarian cancer, Early detection, Targeted ultrasound imaging, $\alpha_v\beta_3$-integrins, animal model

16. SECURITY CLASSIFICATION OF:			17. LIMITATION OF ABSTRACT	18. NUMBER OF PAGES	19a. NAME OF RESPONSIBLE PERSON
					USAMRMC
a. REPORT	b. ABSTRACT	c. THIS PAGE			19b. TELEPHONE NUMBER *(include area code)*
U	U	U	UU	46	

Standard Form 298 (Rev. 8-98)
Prescribed by ANSI Std. Z39.18

Table of Contents

Page

Introduction…….……..…..4

Body……..4

Key Research Accomplishments…….…….. 11

Reportable Outcomes……12

Conclusion……13

References…….13

Appendices……15

INTRODUCTION:

Ovarian cancer (OVCA) remains the most lethal gynecologic malignancy among women. Women with OVCA exhibit specific symptoms only in later stages (Stage III and IV) where the 5-year survival rate is <10% [1, 2]. In contrast, 80-90% OVCA patients detected in stage I respond to treatment[3]. Unfortunately, symptoms of OVCA at the early stage are non-specific and early detection (<25% cases) generally occurs by happenstance[3]. Moreover, the capacity to follow tumor development non-invasively, if it was detected, is non-existent. A valid animal model overcomes the numerous problems associated with clinical studies[4]. Transvaginal ultrasound (TVUS) scanning is the currently favored method for *in vivo* detection of ovarian abnormalities including OVCA. Diagnosis by TVUS scanning is based on the detection of ovarian morphological and vascular abnormalities associated with the disease. However, the detection limits of traditional TVUS do not allow for detection of microvessels at early stages of the disease. Malignant nuclear transformation and changes in nuclear matrix proteins (NMPs) as well as ovarian tumor associated neoangiogenesis (TAN) occur early in OVCA development. Malignant changes in the nucleus are associated with the shedding of NMPs into the circulation which elicits autoimmune responses through production of anti-NMP antibodies. $\alpha_v\beta_3$-integrins and death receptors (DR) 6 are markers of ovarian TAN and are overexpressed by ovarian tumor associated microvessels. In OVCA patients, DR-6 is shed into the circulation. Thus anti-NMP antibodies and DR6 represents potential circulatory markers of malignant ovarian transformation and ovarian TAN. Our long term goal is to improve the TVUS detectability of ovarian TAN vessels at the early stage by molecular targeted ($\alpha_v\beta_3$-integrins) contrast enhanced ultrasound (CE-US) imaging. Contrast agents are developed to improve the visualization of TAN vessels by TVUS scanning. We are using laying hens because of the difficulty in identifying and accessing patients with early stage OVCA.

BODY: the research accomplishments associated with each task outlined in the approved Statement of Work.

Our overall hypothesis is that early stage OVCA lesions can be detected in the hen model using $\alpha_v\beta_3$-integrin targeted CE-US together with anti-NMP antibodies and serum levels of DR6. This hypothesis is being achieved by accomplishing following three specific aims:

Aim 1: To determine whether CE-US using microbubbles targeted to $\alpha_v\beta_3$-integrins will identify hens with ovarian TAN at early stage of OVCA;

Aim 2: To examine whether anti-NMP antibodies appear in serum before ovarian TAN becomes detectable;

Aim 3: To determine whether CE-US indices and serum DR-6 levels established in Specific Aim1 will detect ovarian TAN at early stage OVCA in anti-NMP antibody positive hens.

Accomplishments reported in year-1 (2009-2010):

Task 1. Molecular targeted contrast enhanced ultrasound (CE-US) imaging of hen ovarian tumor associated neo-angiogenesis (TAN)

1a. Scanning of hens by $\alpha_v\beta_3$-integrins targeted contrast enhanced molecular imaging

1) Gray scale scanning: Pre-contrast and post-contrast examination of hen ovaries and recording of still images and video clips.
2) Contrast parameters: Contrast parameters including time of arrival, features of contrast agent binding and wash-out of unbound contrast agents were examined.

3) Doppler ultrasound indices: ovarian vasculature of hens was examined by pre- and post-contrast injection by Doppler ultrasound imaging. Resistive (RI) and pulsatility indices (PI) were recorded.
4) Blood samples: Collected before the injection of contrast agent, sera were obtained and archived.
5) Determination of death receptor (DR6) levels: Serum DR-6 levels were determined by immunoassay.

1b. Following ultrasound scanning, all animals were euthanized and ovaries were collected and processed for paraffin, frozen and molecular biological studies.

1c. Pathology, molecular biology and biochemical study of hen samples:

1. Paraffin and frozen sections from all ovarian tissues blocks from all hens were made and representative sections were stained by hematoxylin & eosin for the diagnosis of tumor or non-tumor abnormalities.
2. Immunostaining of paraffin or frozen ovarian sections for DR-6 and $\alpha_v\beta_3$-integins as well as immunoblotting of ovarian homogenates for the expression of DR-6.
3. Data analysis and establishment of indices for targeted CE-US imaging, RI & PI values and serum DR-6 levels detective of ovarian TAN at early stage OVCA with reference to histopathology and expression of tumor associated angiogenic markers. These indices are being used for the detection of early stage OVCA in subsequent Task (Specific Aim-2).

Accomplishments for the current reporting year (year 2 of the project life, 2010-2011):

Task 2. Appearance of anti-nuclear matrix protein (NMP) antibodies in serum and its association with ovarian TAN in prospective study.

2a. Hens with ovaries appearing normal (with normal egg laying rates and low egg laying rates) were scanned using indices established in Task 1 (specific Aim 1).
2b. Sera of all hens selected by CE-US scan (mentioned in 2a) were examined for the presence of anti-NMP antibodies by immunoassay and hens negative for serum anti-NMP antibodies or hens with normal levels of serum DR6 were selected for specific aim 2. These hens were monitored by CE-US scanning at 15 week intervals for the detection of ovarian TAN at early stage of OVCA. Sera from all hens were collected at each scan and analyzed for the appearance or prevalence of anti-NMP antibodies and DR6 levels.
2c. Hens suspected to have ovarian solid masses and/or ovarian TAN at each scan or all remaining hens at the end of the 45 week monitoring period were euthanized, examined at gross and tissue samples were processed for histopathology, immunohistochemistry including $\alpha_v\beta_3$-integrins and DR6 expression, proteomics and molecular biological examination.
2d. Correlation between serum prevalence of anti-NMP antibodies and DR6 levels with CE-DUS indices diagnostic of OVCA was examined.

Detail Report on the accomplishments for year 2 of the project life (2010-2011):

Specific Aim 2: To examine whether anti-NMP antibodies appear in serum before ovarian tumor associated neo-angiogenesis (TAN) becomes detectable.

Animals: White Leghorn laying hens (3-year old) were examined by $\alpha_v\beta_3$-integrins targeted CE-US imaging using indices established in Specific Aim 1 (reported earlier, RI > 0.44 and PI > 0.96, pixel intensities <18000 pixels) and their sera were tested for the prevalence of anti-NMP antibodies and DR6 levels as reported earlier [5]. A total of 40 hens with normally appearing ovaries (20 with low laying rates and without ovarian TAN and 20 with normal egg laying rates) and negative for serum anti-NMP antibodies as well as with normal DR6 levels were selected. Anti-NMP antibodies in the sera were determined by immunoassay using nuclear matrix

protein extracts from normal or tumor ovaries as reported previously [6]. Hens were monitored for 45 weeks by $\alpha_v\beta_3$-integrins targeted CE-US imaging at 15 week intervals. Sera from all hens were collected at each scan and stored at -80^{0}C .

$\alpha_v\beta_3$-*integrins* targeted contrast enhanced ultrasound (CE-US) imaging:

Scanning of hens and analysis of sonograms were performed similar to *Specific Aim 1* which is briefly mentioned below:

Pre-contrast scanning: Sonography was performed in a continuous pattern before and after the injection of contrast agent with the mechanical set up reported previously [7]. Briefly, all hens were scanned using an instrument equipped with a 5- to 7.5-MHz endovaginal transducer (MicroMaxx; SonoSite, Inc, Bothell, WA). Each hen was immobilized, the transducer was inserted (transvaginally), and a 2-dimensional transvaginal gray scale sonography as well as a pulsed Doppler sonography was performed. The resistive index (RI: [systolic velocity – diastolic velocity]/systolic velocity) and the pulsatility index (PI: [systolic velocity – diastolic velocity]/mean) were automatically calculated from at least 2 separate images from the same ovary, and the lower RI and PI values were used for analysis. All images were processed and digitally archived.

Post-contrast Scanning

Post-contrast injection scanning was performed in a similar and continuous manner with identical mechanical settings as described above and the same pre-contrast imaged area was imaged according to the instruction of the manufacturer of the contrast agent and the earlier report [8]. Within 5-7 min from the arrival of the contrast agent, it accumulated at the target sites and unbound free microbubbles were washed out. All images were archived digitally in a still format as well as real-time clips (15 minutes for each hen). The effect of the contrast agent was evaluated visually during the examination and afterward from reviewing the archived still images and video clips. The time of the contrast agent arrival (interval in seconds from administration of the contrast agent to its visual observation [in seconds]) in the normal and tumor ovaries was recorded in real time. After review of the complete clip, the region of interest (ROI) was selected. The average image intensity over a ROI encompassing the tumor was calculated and normalized by the pre-contrast intensity of the same ROI. The pixel intensity of ROI predictive of OVCA was determined. In addition, post-contrast RI and PI were calculated.

Result: On gray scale sonography at initial scan, healthy hens with low egg laying rates (n = 20 selected hens) showed one or two large preovulatory and several small growing follicles in the ovarian stroma. Blood vessels were detected in the ovarian stroma on color Doppler ultrasound imaging. Overall, similar to previous observation, compared with pre-contrast, the pixel intensity of the signals from the ovary increased significantly after the injection of the contrast agent. No detectable changes or abnormalities in ovarian morphology were observed in any of the experimental hens by targeted imaging at the 1st interval (15 weeks after initial scan). However, at the 2nd interval (30 weeks from initial scan) tumor related changes were suspected in 2 of 20 old hens with low egg laying rates. These morphological changes included a small solid tissue mass-like appearance limited to a part of the ovary with little or no ascitic fluid. Sonograms of these hens were processed and analyzed off-line immediately to determine the signal intensities in pixel values from the ROIs (consisting of the area suspected to have a solid mass) of the images. All of these hens had signal intensities above the pixel values indicative of tumor established in Specific Aim 1. These hens were euthanized and processed for subsequent tissue and molecular studies mentioned later. **Figure 1** shows representative ultrasound images of an ovary before and after the injection of $\alpha_v\beta_3$-integrins targeted contrast agent (B-mode, showing tumor size and borders). Post-contrast imaging predicted to have a small solid mass. At 3rd scan (45 weeks from the initial scan), 6 of the remaining 18 hens were diagnosed with ovarian tumor related changes. These 6 hens together with the remaining 12 hens with apparently normal ovaries were euthanized at the end of the 45 weeks. Thus, compared to pre-contrast scans, targeted imaging by $\alpha_v\beta_3$-integrins targeted contrast agent enhanced

visualization of solid masses in the ovaries of 8 hens on gray scale. All hens that developed ovarian tumors later showed a consistent decrease in RI and PI values even before the tumor become detectable (**Figure 2**). The post-contrast RI and PI values for all of these hens with detectable solid ovarian mass were <0.44and <0.96, respectively as determined in Specific Aim 1. All hens with RI values less than 0.44 were predicted to have ovarian TAN based on their ovarian vascularity as depicted by Doppler ultrasound scan following the targeted imaging.

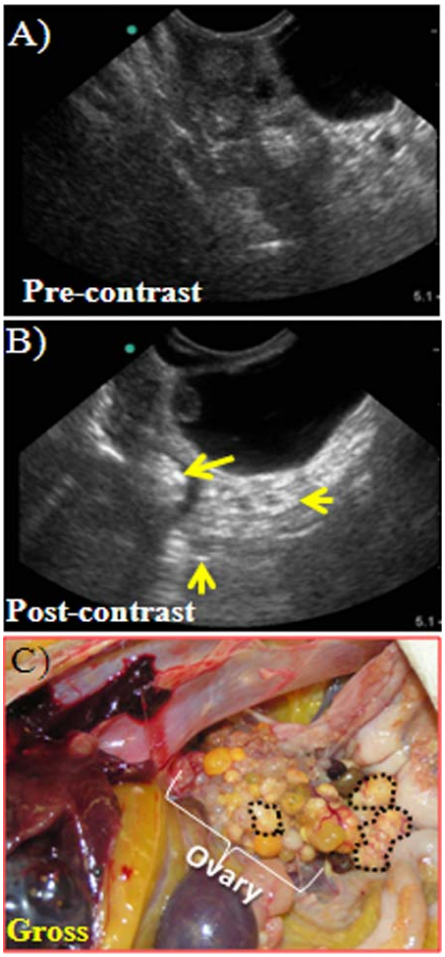

Figure1. $\alpha_v\beta_3$-integrins targeted molecular imaging probes enhanced the detection of spontaneous ovarian tumors in hens. A) Pre-contrast gray scale ultrasound image of a hen ovary showing low signal intensity from the tissue making the detection of any solid mass difficult. B) Post-contrast gray scale targeted imaging of the same ovary showing the enhancement of the ultrasound signal intensity indicative of solid tissue mass. Arrows indicate the examples of specific bindings of imaging agents with the targets. C) Gross appearance of ovarian tumor diagnosed at early stage in (B). Tumor masses are limited to a part of the ovary (black dotted circles).

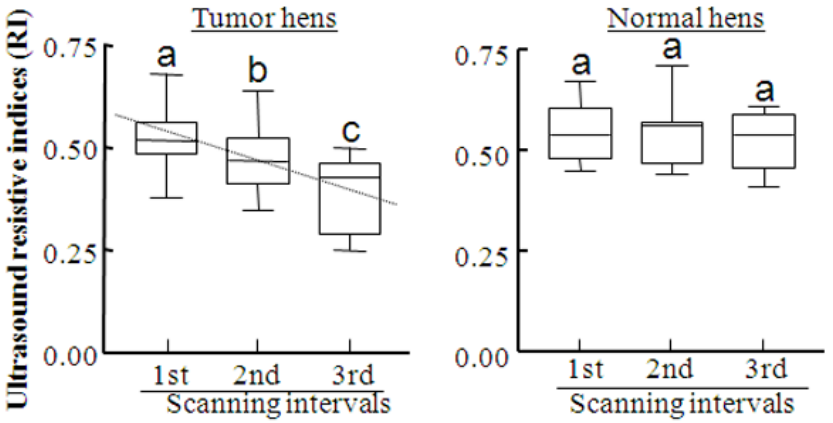

Figure 2. Changes in ultrasound resistive indices (RI) in association with ovarian tumor development in hens displayed as box and whiskers. The median, range (whiskers), and 25th to 75th percentiles (box) are shown. Hens were monitored prospectively by $\alpha_v\beta_3$-integrins targeted ultrasound imaging at 15 week intervals. RI values in hens (that developed tumors later) reduced consistently (P <0.001) from 1st scan to 3rd scan at the time of OVCA diagnosis (left panel, an imaginary dotted line shows the gradual reduction). Reduced RI values indicate lower resistance causing the increases flow of blood to the tissue, a characteristics feature associated with tumor development. Similar patterns of changes were also observed for PI values. However, such consistent changes in RI values were not observed in hens remaining normal. Bars with different letters indicate significant differences within the same group.

Gross and histopathologic evaluation

All hens suspected of ovarian tumors and those remaining apparently normal during scanning by $\alpha_v\beta_3$-integrins targeted contrast agent at different intervals including the final one at the end of the 45-weeks of prospective monitoring were euthanized. Gross ovarian morphology and stages of OVCA were recorded, normal ovaries and ovaries with tumor were harvested and processed for histopathological and immunohistochemical studies (paraffin and frozen), proteomic and molecular biological studies. Ovarian tumors, their stages, and types were confirmed by routine histologic examination with hematoxylin-eosin staining (**Figure 3A-B**). Predictions of targeted imaging were compared and confirmed by gross examination of hens at necropsy and from routine histology. As observed on sonography, ovarian tumors (n = 8 hens) were limited to the ovary (3 serous, 4 endometrioid, and 1 mucinous) with little or no ascites.

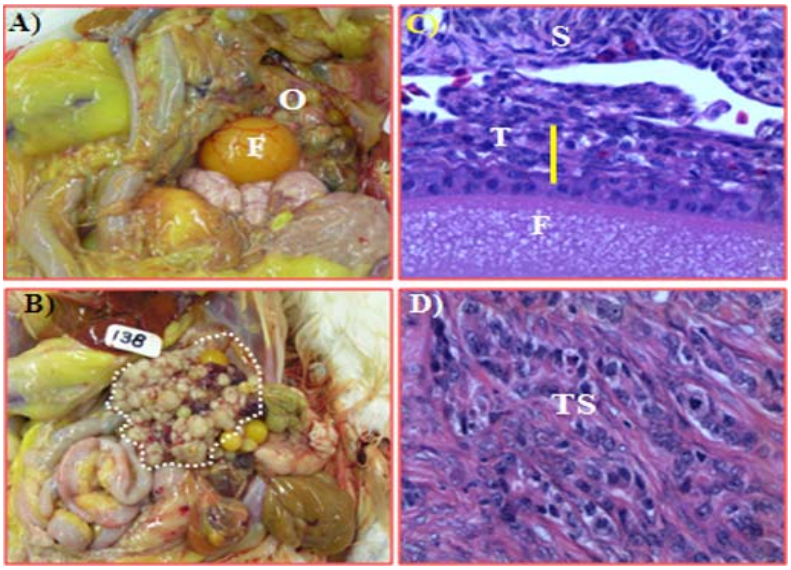

Figure 3. Spontaneous ovarian tumors in laying hens diagnosed by $\alpha_v\beta_3$-integrins targeted ultrasound molecular imaging. A) A normal ovary in an old laying hen with low egg laying rates showing a preovulatory follicle in the ovary. B) An ovarian tumor at early stage in a laying hen. The tumor is limited to the ovary and appears like a cauliflower. Dotted line shows the tumor. C) Section of a normal ovary showing a growing follicle embedded in the ovarian stroma. D) Section of a serous ovarian carcinoma appearing like a sheet of malignant cells with pleomorphic nuclei surrounded by fibromuscular layer. F=follicle, O=ovary, S=stroma, T=theca layer, TS=tumor stroma. H&E, 40X.

NMP antibodies. Anti-NMP antibodies are well established markers for several human autoimmune diseases and are associated with carcinoma of several organs.

Circulating anti-NMP antibodies were detected as reported previously with a little modification [6]. 96-well immunoassay plates were coated with tumor NMPs from hens with OVCA, overnight blocked and incubated with serum from normal or hens with OVCA for two hours followed by rabbit anti-chicken alkaline phosphatase conjugated second antibodies for one hour. Immunoreaction was developed using alkaline phosphates substrate and plates were read at 405nm and optical density (OD) values were recorded. 5 young laying hens with normal egg laying rates were used as controls. Mean OD + 3SD of control hens were used as cut-off values. Hens with OD values greater than the

Association of serum prevalence of anti-NMP antibodies and DR6 levels with the development and progression of ovarian tumors:

Blood from all hens was collected prior to ultrasound scanning and serum samples in aliquots were stored at -80^{0}C until further use. Serum samples were used in immunoassay for the detection of anti-NMP antibodies and DR6 as well as in immunoproteomics for confirming the immunoreactivities of serum against the ovarian tumor NMPs.

Prevalence of anti-NMP antibodies in serum: The nucleus of the cell has long been used in the pathological diagnosis of cancer. Tumor associated changes in the molecular and morphological features of the nucleus represent the earliest event leading to malignant differentiation of the cell. Enlargement in size and irregular shape of the nucleus, re-organization of the chromatin and modifications in the composition of the nuclear matrix (which organizes the chromatin within the nucleus) are changes associated with malignant nuclear transformation. These morphological changes lead to the shedding or release of nuclear matrix proteins (NMPs) into the circulation eliciting an autoimmune response producing anti-

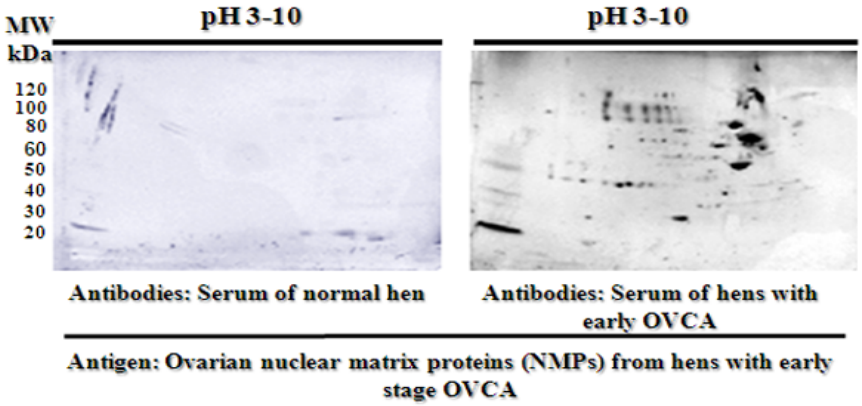

Figure 4. Immunoproteomic detection of anti-NMP antibodies in serum of hens with or without OVCA. Membranes containing nuclear matrix proteins (NMPs) from ovarian tumor were reacted against normal and OVCA sera and immunostained for the detection of serum immunoreactivities for anti-NMP antibodies by 2dimensional Western blotting (2D-WB). Compared with serum from normal hens (left panel), serum from hens with OVCA reacted specifically against the ovarian NMPs from OVCA hens. The size of the reactive antigens mostly ranged from 30-80kD.

cut-off value were considered as positive for circulating anti-NMP antibodies. At the 1st interval (15 weeks after initial scan), 3 of 20 hens were found positive and additional 4 hens were positive at the 2nd interval (30 weeks after initial scan) and 4 of remaining 13 hens were positive for anti-NMP antibodies at the final scan (45th weeks after the initial scan). Thus a total of 11 of 20 hens had anti-NMP antibodies in their serum at the end of 45 week of monitoring. Once a hen became positive for anti-NMP antibodies it remained positive for subsequent intervals. All hens with OVCA were positive for serum anti-NMP antibodies. Immuno-proteomic analysis (two-dimensional Western blotting) using representative sera positive for anti-NMP antibodies showed specific immunoreactivity of tumor sera against tumor NMPs (**Figure 4)**.

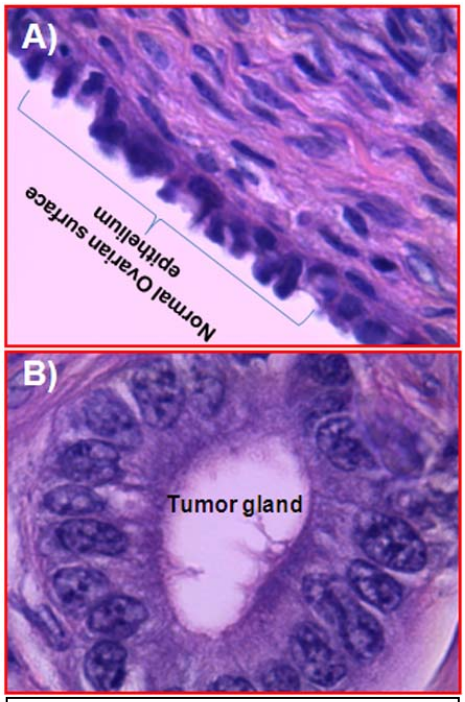

Figure 5. Changes in nuclear morphology of ovarian surface epithelial cells during malignant transformation. A) Section of a normal ovary showing ovarian surface epithelial cells with small and cuboidal or oval shaped nuclei. B) Ovarian section from a hen at early stage OVCA (containing a small tumor mass limited to a part of the ovary) and positive serum anti-NMP antibodies. Compared to normal, the nuclei increased in size and changed in shape (irregular) during malignant transformation. The nuclei become pleomorphic with mitotic bodies. H&E, 100X.

Changes in nuclear morphology are shown in **Figure 5**. Nuclear areas in normal or malignant cells were counted from 5 random fields at 100X in section stained with hematoxylin and eosin. The Mean (+SD) area (expressed in μm^2) of the 5 largest nuclei were counted from a 100X light microscopic, filed and the mean of 5 fields were considered as the mean area of the nucleus in a normal or malignant ovarian section. The average of 3 sections from the same ovary was considered as the mean area of the nucleus of a hen with or without OVCA. 8 hens with OVCA (3 serous, 4 endometrioid and 1 mucinous) and 8 normal hens were used for nuclear morphometric analysis. As compared with the mean area of the nuclei in normal hens, the mean area of the nuclei was significantly greater in hens with OVCA or hens positive for serum anti-NMP antibodies (**Figure 6**). A nuclear morphological index (NMI) = nuclear area (NA) in (OVCA hens)/ (NA in control hens) was determined and a cut-off value (>2X NA of normal hens) was found diagnostic of OVCA based on tumor histopathology. These results suggest that malignant nuclear transformation is associated with the prevalence of anti-tumor antibodies in serum.

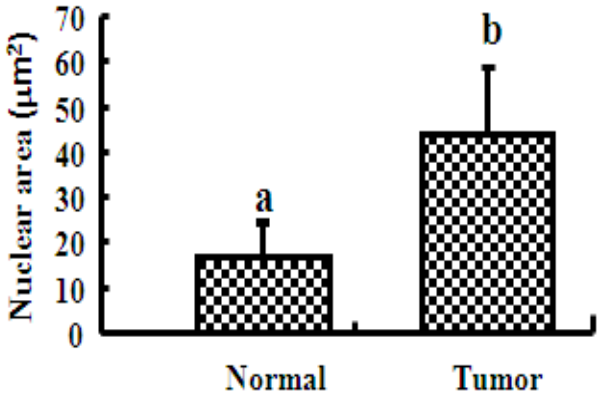

Figure 6. Changes in nuclear size during malignant cellular transformation in the ovary of hens. Nuclear area is expressed as mean + SD in μm^2 (n =8). Compared with normal ovarian surface epithelium, the nuclear area of malignant cells was significantly ($P<0.01$) greater in hens with early stage OVCA (n =8) than in normal hens. (n = 8). Bars with different letters indicate significant differences.

Association of DR6 levels with ovarian tumor development:

Death receptor (DR) 6 is a member of the tumor necrosis factor super family receptor associated with the induction of apoptosis under normal conditions. In contrast, apoptosis in ovarian tumors is reduced although DR6 expression is remarkably higher than in normal ovaries. DR6 is expressed in tumor cells and in the endothelium of tumor microvessels and is associated with malignant progression in human OVCA. DR6 has been reported to be expressed in the laying hen ovary and shown to induce apoptosis in granulosa and theca cells of ovarian follicles. Importantly, the expression of DR6 by reproductive tissues that exhibit increased physiological

angiogenesis, such as placenta, corpus luteum, or proliferative endometrium are significantly less as compared with tumor tissues.

DR6 levels in the sera of normal or OVCA hens were determined by immunoassay using anti-chicken DR6 antibodies. Hens with optical density (OD) values for serum DR6 level greater than a cut-off value established in Specific Aim 1 (mean OD of normal hens + 3SD, 3.02 + 0.06 X 3=3.20) were considered to have OVCA. Hens with OD values for serum DR6 levels greater than the cut-off value were considered to have ovarian tumor associated neo-angiogenesis (TAN). All hens predicted to have ovarian tumors or ovarian TAN by the CE-DUS imaging had OD values for DR6 higher than the OVCA diagnostic level established in Aim 1 (mean + SD = 3.02 + 0.06 X 3=3.20). Immunoreactivity of DR6 proteins was confirmed by immunoblotting using selected serum samples. These results suggest that the development of ovarian tumors is associated with an increase in serum levels of DR6.

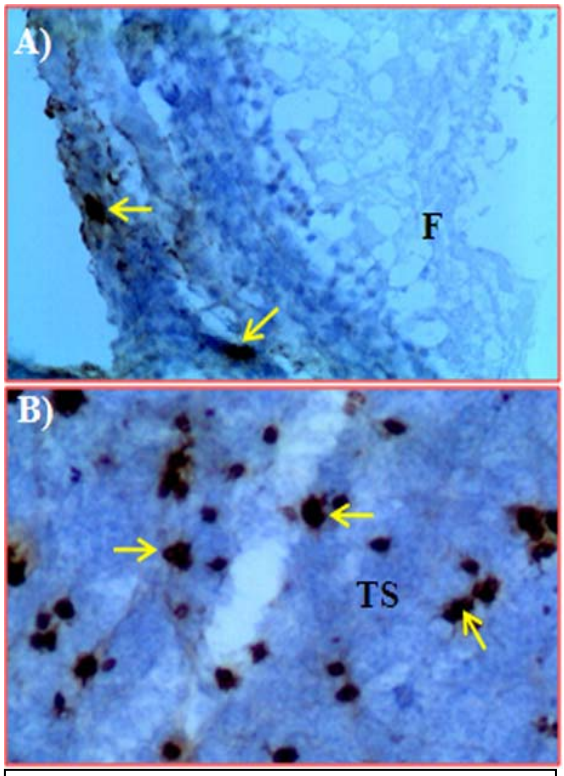

Figure 7. Immunohistochemical detection of $\alpha_v\beta_3$-integrins expressing microvessels in the stroma of a normal ovary or ovary with tumor at early stage in hens. Sections were immunostained with anti-$\alpha_v\beta_3$-integrins antibodies. Compared with normal ovary (A), more $\alpha_v\beta_3$-integrins expressing microvessels are seen in the stroma of the ovaries with early stage OVCA (B). Arrows indicate the examples of immunopositive microvessels. F = stromal follicle, TS = tumor stroma. 40X.

Tissue expression of markers of ovarian tumor associated neo-angiogenesis (TAN):

Expression of $\alpha_v\beta_3$-integrins and DR6 by normal ovaries and ovaries with tumor was determined by immunohistochemistry using anti-DR6 and anti- $\alpha_v\beta_3$ integrins antibodies. Immunopositive microvessels or cells were counted as reported previously [9].

Expression of $\alpha_v\beta_3$-integrins: $\alpha_v\beta_3$-integrins were expressed by the endothelium of the immature and leaky angiogenic microvessels and localized at the tumor vicinity (spaces between tumor glands) (**Figure 7**) with occasional expression by ovarian epithelia. Compared to normal hens (**Figure 7A**), the frequencies of $\alpha_v\beta_3$- integrin expressing microvessels were significantly ($P<0.05$) greater in hens with early stage OVCA (mean + SD= 5.84 + 1.66 in 20,000μm^2 of tumor tissue) than normal hens (2.92 + 0.90 in 20,000μm^2 of ovarian stromal tissue) (**Figure 7B**). These results confirm that the greater signal intensities from hens with suspected ovarian tumor mass observed in the molecular targeted CE-US imaging suggest that ovarian tumor associated microvessels express $\alpha_v\beta_3$-integrins which can be detected *in vivo* and may be used as an imaging marker for the detection of OVCA at the early stage.

Tissue expression of DR6: Malignant ovarian tumor epithelium in OVCA hens as well as angiogenic microvessels was positive for DR6 expression (**Figure 8**). In normal ovaries, few microvessels in the follicular theca and in the stroma showed immunoreactivities for DR6 (2.81 + 0.56 in 20,000μm^2 of ovarian stromal tissue) while many DR6+ microvessels were localized in hens with early stage OVCA (mean + SD= 6.44 + 0.66 in 20,000μm^2 of tumor tissue, $P<0.05$) (**Figure 9**).

Tumor associated neo-angiogenic index (TANI) diagnostic of OVCA established in Specific Aim 1 (TANI = Ti/ Ni + T_d/N_d; where Ni & Ti and N_d & T_d are the number of $\alpha_v\beta_3$-integrins and DR-6 positive

vessels in normal and tumor hens, respectively) were evaluated for the detectability of ovarian TAN. TANI for normal ovary was considered as 2 (1 for $\alpha_v\beta_3$-integrins and 1 for DR-6 expressing vessels). Values of TANI from all hens at early stage OVCA were greater than normal hens (4.30 vs 2, P <0.01).

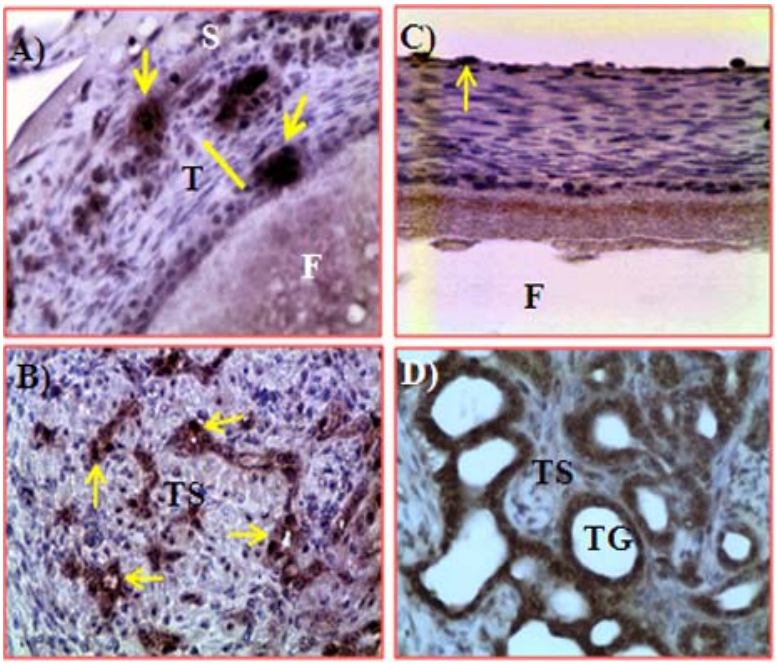

Figure 8. Immunohistochemical detection of DR6 expression in normal ovaries or ovaries with tumor. Sections were immunostained with anti- chicken DR6 antibodies. A-B*) DR6 expression by microvesse*ls in the stroma of a normal ovary (A) or ovary with tumor at early stage (B) in hens. Compared with norrmal ovary (A), more DR6 expressing microvessels are seen in the stroma of the ovaries with early stage OVCA (B). C-D) *DR6 expression by ovarian malignant epithelial cells*. Very few normal ovarian surface epithelium expressed DR6 (C). Compared with normal, strong immunoreaction was detected in malignant epithelium (D). Arrows indicate the examples of immunopositive microvessels or epithelial cells. F = stromal follicle, TG = tumor gland, TS = tumor stroma, 40X.

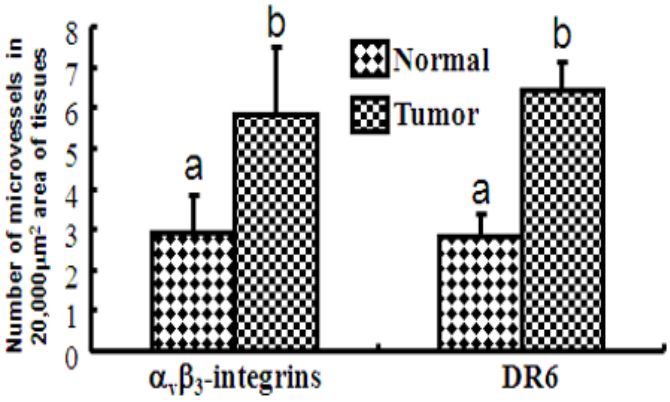

Figure 9. Changes in the frequencies of $\alpha_v\beta_3$-integrins and DR6 expressing microvessels in association with ovarian tumor development in hens. The numbers of immunopositive microvessels are expressed as mean + SD. Compared with normal hens (n = 11), the number of $\alpha_v\beta_3$-integrins and DR6 expressing microvessels was significantly (P <0.01) greater in OVCA hens (n= 8) than normal hens. Bars with different letters indicate significant differences.

As a whole, Specific Aim 2 showed that (1) serum anti-NMP antibodies appear before the tumor becomes detectable by targeted ultrasound imaging, positively correlated with the malignant nuclear transformation and ovarian TAN; (2) Serum prevalence of anti-NMP antibodies is correlated with the serum levels of DR6 detective of OVCA or ovarian TAN.

KEY RESEARCH ACCOMPLISHMENTS:

The key research accomplishments during the reporting period are:

- Established that ovarian tumor associated anti-NMP antibodies appear in serum before the tumor becomes detectable by targeted ultrasound imaging;
- Serum anti-NMP antibodies are an indicator of ovarian malignant nuclear transformation;
- Prevalence of serum anti-NMP antibodies is associated with the increase in serum DR6 levels detective of OVCA;

- ❖ Prevalence of serum anti-NMP antibodies is associated with changes in targeted ultrasound signal intensities relative to ovarian tumor development;
- ❖ Ovarian tumor associated neoangiogenic changes are associated with the prevalence of anti-NMP antibodies in serum;
- ❖ The indices for targeted ultrasound imaging diagnostic of OVCA including signal intensities, index for ovarian TAN and serum DR6 levels diagnostic of OVCA detected OVCA successfully.

REPORTABLE OUTCOMES:

Manuscript: *In press* or Published

1. **Barua A**, Yellapa A, Bahr JM, Abramowicz JS, Edassery SL, Basu S, Rotmensch J and Bitterman P (**2012**). Expression of death receptor 6 (DR6) by ovarian tumors in laying hens, a preclinical model of spontaneous ovarian cancer, *Translational Oncology, In press* (Volume 5, Issue 4, PP XX). http://www.transonc.com/future.php?vol=5&no=4 (***Appended at pages 15-23***)

2. Khan M, Bahr JM, Yellapa A, Bitterman P, Abramowicz JS, Edassery SL, Basu S, Rotmensch J and **Barua A** (**2012**): Expression of Leukocyte Inhibitory Immunoglobulin-like Transcript 3 Receptors by Ovarian Tumors in Laying Hen Model of Spontaneous Ovarian Cancer, *Translational Oncology*, 2012 April; 5(2): 85–91. PMID: 22496924 (***Appended at pages 24-30***)

3. Yellapa A, Bahr JM, Bitterman P, Abramowicz JS, Edassery SL, Penumatsa K, Basu S, Rotmensch J and **Barua A** (**2012**). Association of Interleukin 16 with the development of ovarian tumor and tumor associated neo-angiogenesis in laying hen model of spontaneous ovarian cancer *International Journal of Gynecological Cancer,* 22(2):199-207. PMID: 22274315 (***Appended at pages 31-39***)

Presentation: Abstract published and presented (***link provided***):

1. **A. Barua**, A. Yellapa, P. Bitterman, J. M. Bahr, S. Sharma, D. B. Hales, J. L. Luborsky, J. S. Abramowicz (2011): Use of contrast-enhanced ultrasound imaging with microbubbles targeted to $\alpha_v\beta_3$ integrins to enhance detection of early-stage ovarian tumors, ASCO Annual Meeting. Chicago, IL, USA; June 3-7, 2011. (***Appended at pages 40-41***)

   http://www.asco.org/ascov2/Meetings/Abstracts?&vmview=abst_detail_view&confID=102&abstractID=84636

2. Aparna Yellapa, Jacques S. Abramowicz, Pincas Bitterman, Janice M. Bahr, Michael J. Bradaric, Seby L. Edassery, Sameer Sharma, **Animesh Barua**. Interleukin (IL-16) and tumor associated neo-angiogenesis detects ovarian cancer at early stage. AACR 102th Annual Meeting, Orlando, FL, April 2-6, 2011. (***Appended at page 42***)
   http://www.abstractsonline.com/Plan/ViewAbstract.aspx?sKey=0732f136-3e77-422d-886b-29769face7da&cKey=fc49e373-cefe-430d-ae3f-058a41a93bf4&mKey=%7b507D311A-B6EC-436A-BD67-6D14ED39622C%7d
3. Yellapa A, Khan MF, Bahr JM, Bitterman P, Abramowicz JS, Basu S, Edassery SL, **Barua A.** (2012). Expression of death receptor 6 (DR6) increases in association with ovarian tumor development and

progression. In: Proceedings of the 103rd Annual Meeting of the American Association for Cancer Research; 2012 Mar 31-Apr 4; Chicago, IL. Philadelphia (PA): AACR; Cancer Res 2012; 72(8 Suppl): Abstract nr 3646. doi:1538-7445.AM2012-3646 (***Appended at page 43***)
http://cancerres.aacrjournals.org/cgi/content/meeting_abstract/72/8_MeetingAbstracts/3646

4. Khan MF, Yellapa A, Bahr JM, Bitterman P, Abramowicz JS, Basu S, Edassery SL, **Barua A.** (2012). Expression of immunosuppressive leukocyte inhibitory immunoglobulin like transcript 3(ILT3) receptors increases with the development and progression of ovarian tumors. In: Proceedings of the 103rd Annual Meeting of the American Association for Cancer Research; 2012 Mar 31-Apr 4; Chicago, IL. Philadelphia (PA): AACR; Cancer Res 2012; 72(8 Suppl): Abstract nr 5415. doi:1538-7445.AM2012-5415 (***Appended at pages 44***)

   http://cancerres.aacrjournals.org/cgi/content/meeting_abstract/72/8_MeetingAbstracts/5415
5. **Barua A**. Molecular targeted ultrasound imaging of $\alpha_v\beta_3$-integrins expressing microvessels in association with anti-NMP antibodies detects ovarian cancer at early stage. **Oral presentation-** *symposium on Ovarian Cancer: Prevention, Detection, & Treatment of the Disease and Its Recurrence: Molecular mechanism and Personalized Medicine, held from May 10-11, 2012, University of Pittsburgh School of Medicine, Pittsburgh, Pennsylvania.* (***Appended at pages 45***) *http://www.upci.upmc.edu/ovarian/index.cfm*

Manuscript in preparation: One manuscript is being submitted

CONCLUSION:

The results of the accomplishments of Aim 1 and Aim 2 suggest that contrast enhanced molecular imaging targeting ovarian $\alpha_v\beta_3$-integrins can detect ovarian tumor associated neo-angiogenesis at early stage ovarian cancer in the laying hen model of spontaneous ovarian cancer. Changes in early stage ovarian cancer related CE-US imaging indices were associated with the elevation of serum levels of death receptor (DR6). Serum prevalence of anti-NMP antibodies is associated with tumor development and progression. Anti-NMP antibodies appear in serum before the tumor become detectable through imagining. Thus serum anti-NMP antibodies may be used as a surrogate marker of ovarian malignant nuclear transformation.

REFERENCES:

1. Goodman MT, Correa CN, Tung KH, Roffers SD, Cheng Wu X, Young JL, Jr., Wilkens LR, Carney ME, and Howe HL. Stage at diagnosis of ovarian cancer in the United States, 1992-1997. *Cancer* 2003; 97: 2648-59.
2. Siegel R, Ward E, Brawley O, and Jemal A. Cancer statistics, 2011: the impact of eliminating socioeconomic and racial disparities on premature cancer deaths. *CA Cancer J Clin*; 61: 212-36.
3. Ries LA. Ovarian cancer. Survival and treatment differences by age. *Cancer* 1993; 71: 524-9.
4. Vanderhyden BC, Shaw TJ, and Ethier JF. Animal models of ovarian cancer. *Reprod Biol Endocrinol* 2003; 1: 67.

5. Barua A, Edassery SL, Bitterman P, Abramowicz JS, Dirks AL, Bahr JM, Hales DB, Bradaric MJ, and Luborsky JL. Prevalence of antitumor antibodies in laying hen model of human ovarian cancer. *Int J Gynecol Cancer* 2009; 19: 500-7.
6. Yu E, Lee H, Oh W, Yu B, Moon H, and Lee I. Morphological and biochemical analysis of anti-nuclear matrix protein antibodies in human sera. *J Korean Med Sci* 1999; 14: 27-33.
7. Barua A, Abramowicz JS, Bahr JM, Bitterman P, Dirks A, Holub KA, Sheiner E, Bradaric MJ, Edassery SL, and Luborsky JL. Detection of ovarian tumors in chicken by sonography: a step toward early diagnosis in humans? *J Ultrasound Med* 2007; 26: 909-19.
8. Anderson CR, Hu X, Zhang H, Tlaxca J, Decleves AE, Houghtaling R, Sharma K, Lawrence M, Ferrara KW, and Rychak JJ. Ultrasound molecular imaging of tumor angiogenesis with an integrin targeted microbubble contrast agent. *Invest Radiol*; 46: 215-24.
9. Barua A, Bitterman P, Bahr JM, Bradaric MJ, Hales DB, Luborsky JL, and Abramowicz JS. Detection of tumor-associated neoangiogenesis by Doppler ultrasonography during early-stage ovarian cancer in laying hens: a preclinical model of human spontaneous ovarian cancer. *J Ultrasound Med* 2010; 29: 173-82.

Translational Oncology
www.transonc.com

Volume 5 Number 4 August 2012 pp. 260–268 260

Expression of Death Receptor 6 by Ovarian Tumors in Laying Hens, a Preclinical Model of Spontaneous Ovarian Cancer[1]

Animesh Barua*,†,‡, Aparna Yellapa*, Janice M. Bahr§, Jacques S. Abramowicz†, Seby L. Edassery*, Sanjib Basu¶, Jacob Rotmensch† and Pincas Bitterman‡

*Department of Pharmacology, Rush University Medical Center, Chicago, IL; †Department of Obstetrics and Gynecology, Rush University Medical Center, Chicago, IL; ‡Department of Pathology, Rush University Medical Center, Chicago, IL; §Department of Animal Sciences, University of Illinois at Urbana-Champaign, Urbana, IL; ¶Department of Preventive Medicine (Biostatistics), Rush University Medical Center, Chicago, IL

Abstract

Tumor-associated neoangiogenesis and suppression of antitumor immunity are hallmarks of tumor development and progression. Death receptor 6 (DR6) has been reported to be associated with suppression of antitumor immunity and tumor progression in several malignancies. However, expression of DR6 by malignant ovarian epithelial tumors at an early stage is unknown. The goals of this study were to determine whether DR6 is expressed by malignant ovarian epithelial tumors at an early stage and to examine whether DR6 expression is associated with ovarian cancer (OVCA) progression in a laying hen model of spontaneous OVCA. Expression of DR6 was examined in normal and malignant ovaries, normal ovarian surface epithelial (OSE) cells, or malignant epithelial cells and in serum of 3-year-old hens. The population of microvessels expressing DR6 was significantly higher in hens with early-stage OVCA than hens with normal ovaries ($P < .01$) and increased further in late-stage OVCA. The results of this study showed that, in addition to microvessels, tumor cells in the ovary also express DR6 with a significantly higher intensity than normal OSE cells. Similar patterns of DR6 expression were also observed by immunoblot analysis and gene expression studies. Furthermore, DR6 was also detected in the serum of hens. In conclusion, DR6 expression is associated with OVCA development and progression in laying hens. This study may be helpful to examine the feasibility of DR6 as a useful surrogate marker of OVCA, a target for antitumor immunotherapy and molecular imaging and thus provide a foundation for clinical studies.

Translational Oncology (2012) 5, 260–268

Introduction

Ovarian cancer (OVCA) is the most lethal tumor among gynecologic malignancies, with an estimated yearly incidence rates of 22,000 in the United States and 42,000 in Europe [1,2]. In most cases, OVCA is detected at advanced stages, and despite the remarkable improvements in treatment strategies, most of these patients have recurrences. The reasons for failure to detect and treat OVCA at an early stage as well as its high rate of recurrences are the lack of an effective early detection test, suppression of antitumor immunity by the tumor, and resistance to drugs [3–5]. OVCA differs from other malignancies in its specific

Address all correspondence to: Animesh Barua, PhD, Laboratory for Translational Research on Ovarian Cancer, Department of Pharmacology, Room # 410 Cohn Bldg, Rush University Medical Center, 1735 W Harrison St, Chicago, IL 60612.
E-mail: Animesh_Barua@rush.edu

[1]This study was supported by the Idea Development Award from the US Department of Defense (OC no. 093303), the National Cancer Institute Pacific Ovarian Cancer Research Consortium Career Development Program (grant P50 CA83636), and the Elmer Sylvia and Sramek Foundation (USA). The authors declare no actual or potential conflict of interest associated with this study.
Received 5 April 2012; Revised 25 April 2012; Accepted 27 April 2012

DOI 10.1593/tlo.12184

dissemination pattern, which is characterized by tumor spread in a diffuse intrapelvic and abdominal manner [5]. Thus, the local tumor microenvironment including tumor-associated neoangiogenesis and suppression of antitumor immunity play important roles in the development and progression of ovarian tumors. However, the way tumor establishes neoangiogenesis and escapes antitumor immune surveillance is not well understood. Information on factors related to the development of tumor-associated angiogenesis and immune suppression in the tumor microenvironment is important because it may offer opportunities to establish an early detection test as well as targeted antitumor therapy. Death receptor 6 (DR6) has been suggested to be one of such factors because of its expression by blood vessels and its involvement in immunoregulation [6,7].

DR6 is a member of the tumor necrosis factor α receptor superfamily (TNFRSF21) [8,9]. Although DR6 has been shown to be involved in apoptotic cell death, elevated expression of DR6 has been observed in several tumors in humans [10]. DR6 expression was increased in tumor tissues from patients with late-stage prostate and breast cancers compared with its level in normal tissues [10]. Recently, DR6 concentration in the serum has been shown to be elevated in patients with late-stage OVCA [6]. In addition, DR6 has been demonstrated to be expressed by blood vessels in tumor tissues [11]. All these reports suggest that increased DR6 expression is associated with advanced stages of several malignancies including OVCA. However, its association with early-stage OVCA including tumor-associated angiogenesis is not known.

Suppression of antitumor immunity has been suggested as one of the mechanisms of tumor survival and progression [5]. Despite the presentation of antigens by malignant cells, which should induce immune-mediated rejection, spontaneous rejection of established tumor is rare [5]. Inefficient tumor rejection by the immune system is not only a passive result of insufficient effector cells [12,13] because tumors induce immune-suppressive mechanisms that protect them against eradication [3,4]. Compared with other solid tumors, studies on immunosuppression by ovarian tumors are very few. As in other epithelial malignancies, antitumor immune responses were reported to be elicited against ovarian tumors [14–16], but these responses were not effective enough to eliminate bulky tumor [5]. Moreover, the distinctive type of disease dissemination (peritoneal spread and metastasis) makes OVCA unique compared to other solid tumors. Although the precise mechanism(s) of inadequate or defective antitumor immune responses are not well understood, expression or secretion of immunosuppressive factors by the tumor has been suggested as a potential strategy for immune evasion. DR6 has been reported to alter normal differentiation of monocyte to immature dendritic cells rather than mature dendritic cells [17] and immature dendritic cells have been demonstrated to induce tolerance [18]. Furthermore, because of its inhibitory roles in T- and B-cell proliferation and migration, DR6 has been proposed to be immunosuppressive and may be involved in tumor cell survival and immune evasion [7]. However, expression of DR6 by ovarian tumors at early stages as well as inhibition of antitumor immunity by DR6 in OVCA patients is not known.

To develop and improve the efficacy of an antitumor immunotherapy, more insight into the interaction between ovarian cancer (OVCA) and the immune system is needed. Information on DR6 expression by ovarian tumors may lead to the identification of additional targets, which may allow opportunities for developing new therapeutic approaches to inhibit tumor progression. Studies on the immune response against tumors or immune suppression by ovarian tumors at early stages are lacking. Furthermore, if DR6 is expressed by ovarian tumor–associated neoangiogenic microvessels, it may be a useful target for the early detection of OVCA by Doppler ultrasound imaging. The difficulty in identifying patients with OVCA at an early stage and the limited access to tumor tissue are significant barriers to the study and to the development of an effective immunotherapy against OVCA. Laying hens are the only widely available and easily accessible animals that develop OVCA spontaneously with high incidence rates and remarkably similar histologic subtypes and tumor markers to human OVCA [19–21]. In addition, avian DR6 has been reported to be orthologous to human DR6 (70% homology) and is expressed by the hen ovaries [22]. Thus, the objective of the present study was to explore whether DR6 is expressed by ovarian tumors in hens and, if so, whether its expression changes in association with the stage of the tumors and histologic subtypes.

Materials and Methods

Animals

A flock of 3-year-old commercial strains of White Leghorn laying hens (*Gallus domesticus*) was maintained under standard poultry husbandry practices. Hens (n = 120) were selected based on their egg laying rates (normal or low) and transvaginal ultrasound scanning as reported previously [23]. The incidence of OVCA in hens of this age group is approximately 15% to 20% and is associated with low or complete cessation of egg laying [19,23]. All experimental procedures were performed according to the institutional animal care and use committee–approved protocol.

Tissue Collection and Processing

Serum samples. Blood was obtained from brachial veins of all hens before euthanasia and centrifuged (1000*g* for 20 minutes), and serum samples were stored at −80°C.

Ovarian morphology and histopathology. Ovarian pathology and tumor staging were performed by gross and histologic examination as reported previously [19]. Each normal and malignant ovary (tumor bearing ovary) was divided into four portions for protein extraction, total RNA collection, paraffin and frozen embedding for routine histology, and immunohistochemical studies as reported previously [24]. Normal ovarian surface epithelial (OSE) cells or tumor cells (malignant epithelial cells of the tumor) in hens with OVCA were collected as reported earlier [25,26]. Samples were divided into three groups including normal and early- and late-stage OVCA based on gross inspection and microscopy as previously reported [19].

Preparation of Ovarian Specimen for Biochemical Analysis

Snap-frozen ovarian tissues as well as normal OSE cells and tumor cells from hens with normal ovaries or hens with OVCA were homogenized with a Polytron homogenizer (Brinkman Instruments, Westbury, NY) as reported previously [27], were centrifuged; the supernatant was collected and the protein content of the extract was measured and stored at −80°C.

Immunohistochemistry

Rabbit polyclonal anti-chicken DR6 antibodies were used as primary antibodies, and immunoreactions were determined using Vectastain Elite ABC kit (Universal, RTU; Vector Laboratories, Inc, Burlingame, CA). Normal or malignant ovaries (n = 15 hens each for normal, early, and late stages) were selected randomly for immunohistochemical study. The number of hens for each group for immunohistochemistry was determined based on the power analysis to achieve significant differences in different parameters among the normal or malignant groups. Briefly, after deparaffinization, antigens on the sections were unmasked by heat treatment, endogenous peroxidase in the sections was inactivated, and nonspecific staining was blocked by incubating with 0.3% hydrogen peroxide in methanol and normal horse serum, respectively. Sections were then incubated for 2 hours with primary antibodies (1:100 dilution) followed by 1 hour of incubation with secondary antibodies (Vectastain Elite ABC kit; Vector Laboratories). Immune reaction products on the sections were visualized by incubating with diaminobenzidine and hydrogen peroxide mixture (DAB Peroxidase Substrate Kit, 3,3′-diaminobenzidine; Vector Laboratories). Sections were then counterstained with hematoxylin, dehydrated, and covered. Control staining was carried out simultaneously in which the first antibodies were omitted and normal serum was used. No staining was found in these control slides.

Sections were then examined under a light microscope attached to digital imaging software (MicroSuite version 5; Olympus Corporation, Tokyo, Japan). The population of microvessels expressing DR6 as well as the intensity of DR6 staining by the normal ovarian stroma or stroma (around the tumor) in malignant ovaries was determined. Three sections per ovary and five regions of interest with the highest immunoreactivity (20,000 μm^2 per region at an objective of ×40 and ocular magnification of ×10) per section were selected. Using the software, the intensity of the DR6 immunostaining in each region was measured and recorded as pixel values in 20,000 μm^2 of the section as reported previously [28]. The mean of pixel values of these five regions in a section was considered as the intensity of DR6 in a 20,000-μm^2 area of each section. The mean intensity of three sections was considered as the DR6 staining intensity in a 20,000-μm^2 area of each normal or malignant ovary. The groupwise DR6 staining intensity (normal or tumor groups) was expressed as mean ± SD in a 20,000-μm^2 area of ovaries in normal or malignant groups. Similarly, and using the same software, the population of microvessels expressing DR6 in the section was counted and reported as the frequency (mean ± SD) of DR6-expressing microvessels in a 20,000-μm^2 area of the stroma of normal or malignant ovaries as reported previously [29].

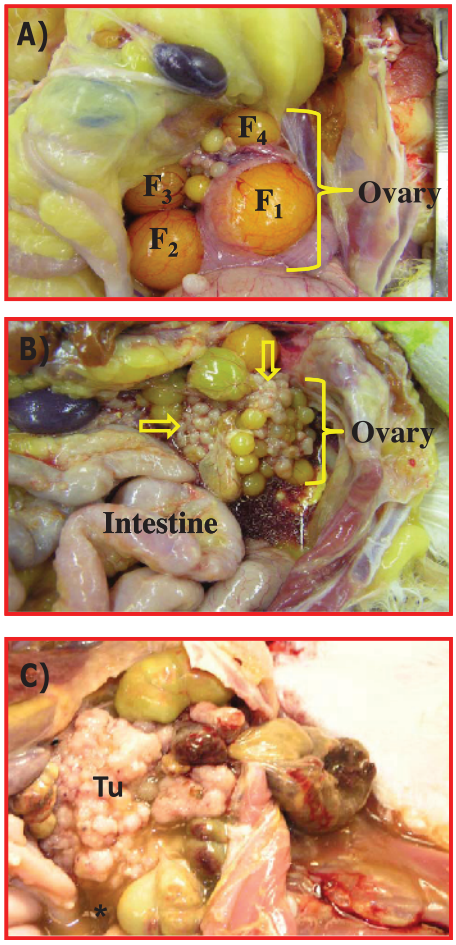

Figure 1. Gross morphology of normal and malignant ovaries in laying hens. (A) Fully functional normal ovary in a laying hen. Laying hens ovulate and subsequently lay eggs once a day for 5 or 6 days in a week in a continuous manner and then take a pause for 1 day before laying resumes. Thus, the ovary in a fully functional laying hen contains a set of multiple large and growing preovulatory follicles arranged in a hierarchy of sizes (F1-F5). The largest follicle (F1) is destined to ovulate soon and then the second largest follicle (F2) becomes F1 and a small growing follicle is recruited from the ovarian stroma to the hierarchy to maintain the laying rates. (B) Ovarian tumor at an early stage in a hen showing solid tumor mass (arrows) limited to the ovary. (C) Ovarian tumor at a late stage. The tumor (Tu) appears like a cauliflower and has metastasized to other organs with accompanied profuse ascites (*).

One-dimensional Western Blot

Ovarian expression of DR6 was confirmed by immunoblot analysis using homogenates of normal (n = 5) or malignant ovaries as well as normal OSE cells or tumor cells. Twelve samples (four from each of the serous, endometrioid, and mucinous samples) at early and late stages of OVCA were selected for immunoblot analysis based on their immunoreactivity for DR6 in immunohistochemistry. Immunoreactions on the membrane were visualized as a chemiluminescence product (Super Dura West substrate; Pierce/Thermo Fisher, Rockford, IL), and the image was captured using a Chemidoc XRS (Bio-Rad, Hercules, CA). Similarly, serum samples from the same hens used for ovarian DR6 expression were selected for immunoblot analysis to examine the presence of DR6 in serum. Serum samples were filtered by acetonitrile and chloroform-methanol precipitation before using for immunoblot analysis [27].

Reverse Transcription–Polymerase Chain Reaction

DR6 mRNA expression was assessed by semiquantitative reverse transcription–polymerase chain reaction (RT-PCR) as reported previously [30]. For RT-PCR analyses, serum and tissue samples from 5 hens with normal ovaries, from 12 hens with early stages of OVCA (4 for each histologic subtype), and from 12 hens with late stages of OVCA (4 for each histologic subtype) were selected based on their reactivity in immunohistochemistry and immunoblot analysis. Hen-specific DR6 primers were designed by OligoPerfect Designer software (Invitrogen, Carlsbad, CA) using the DR6 sequence from the National Center for Biotechnology Information (accession no. A1980074) as reported earlier [22]. The forward primer was 5′-GAT GGA GGA CAC CAC GCC-3′ and the reverse primer was 5′-TCG GGG TTG AGG ATG TGC-3′. β-Actin was used as the endogenous control, with a forward primer of

TGCGTGACATCAAGGAGAAG and a reverse primer of ATGCCAGGGTACATTGTGGT. The expected base pair size for the DR6 amplicon was 384 bp and that for β-actin was 300 bp. PCR amplicons were visualized in a 3% agarose gel (Pierce/Thermo Fisher) in Tris-acetate-EDTA (TAE) buffer and stained with ethidium bromide. The image was captured using a ChemiDoc XRS system (Bio-Rad).

Statistical Analysis

The differences in the intensity of DR6 immunostaining and the number of microvessels expressing DR6 in normal ovaries and malignant ovaries were assessed by analysis of variance, F tests, and the alternative nonparametric Kruskal-Wallis tests. Subsequently, pairwise comparison between the groups (normal and early- and late-stage OVCAs) by two-sample t tests and alternative Mann-Whitney tests were performed. All reported P values are two-sided, and $P < .05$ was considered significant. Statistical analyses were performed with SPSS (PASW) version 18 software (IBM, Inc, Armonk, NY).

Results

Ovarian Morphology

In laying hens, only the left ovary becomes functional, and the rate of egg production declines with aging. A fully functional ovary contains five to six developing large preovulatory follicles (Figure 1*A*). As the hen ages, the rate of egg production decreases. The ovary of an older (>3 years old) healthy hen with a low rate of egg production contains fewer than three large preovulatory follicles. In apparently healthy hens that have stopped laying eggs, the ovaries were atrophied and the oviducts were smaller. Solid tissue masses either limited to a small part or the entire ovary, with or without ascites, were observed in 12 hens. These hens were diagnosed with early-stage OVCA (Figure 1*B*). In 16 hens, tumor had metastasized to the abdominal organs with moderate to profuse ascites. These hens were diagnosed with late-stage OVCA (Figure 1*C*).

Histopathology. Cortical follicles with or without distinguishable granulosa cell and theca layer were embedded in the ovarian stroma of hens with normal ovaries (Figure 2*A*). Tumors were confirmed in all hens displaying gross ovarian solid masses (12 hens at early stage with solid masses limited to the ovaries or in 16 hens with late-stage OVCA) by routine histology (Figure 2, *B-D*). However, tumor-related microscopic changes (including focal lesions containing large cells with irregular shapes and pleomorphic nuclei) were also found during histologic examinations in 11 additional hens that had no gross ovarian tumor and were grouped in early-stage OVCA. Thus, a total of 23 (12 + 11) hens had early-stage OVCA, 16 had late-stage OVCA, whereas 81 hens had normal ovaries. Tumors were typed as serous (n = 17), endometrioid (n = 12), mucinous (n = 8), clear cell (n = 1), as well as mixed (n = 1, seromucinous) as reported previously [19].

Tissue Expression of DR6

Microvessels expressing DR6 were detected in both normal and malignant ovaries (Figure 3). Most of the DR6-expressing ovarian

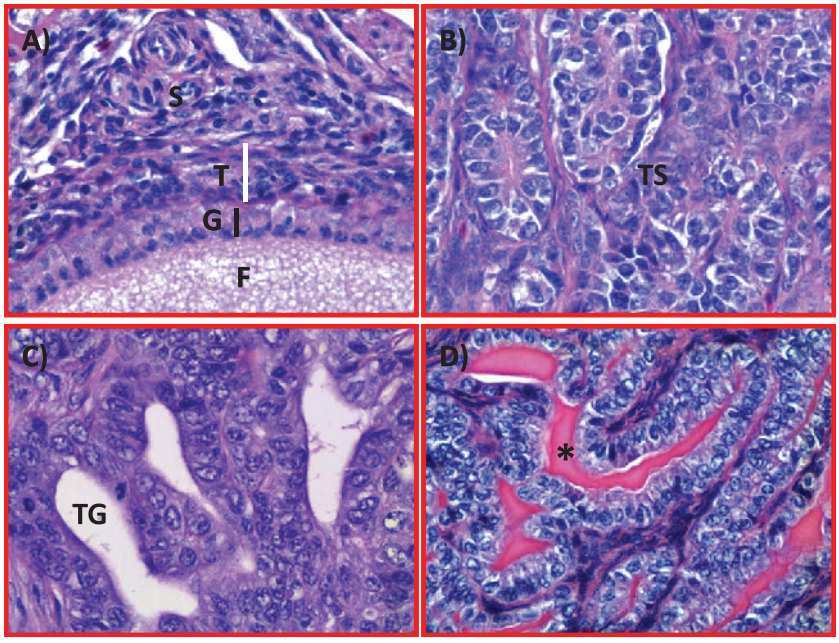

Figure 2. Microscopic features of hen ovaries. Paraffin-embedded sections from normal or malignant ovaries with tumors were stained with hematoxylin and eosin. (A) Section of a normal ovary showing a developing follicle embedded in the ovarian stroma. (B) Section of an ovarian serous carcinoma showing a solid sheet of tumor surrounded by fibromuscular tissue. The tumor contains a labyrinth of slitlike glandular spaces lined by cells with large pleomorphic nuclei and mitotic figures. (C) Section showing endometrioid carcinoma displaying confluent back-to-back glands. Glands contain a single layer of epithelial cells with sharp luminal margins. (D) Section of a mucinous carcinoma. Glands in clusters with scarce intervening stroma lined by columnar and goblet cells with intracytoplasmic mucin. Original magnification, ×40.

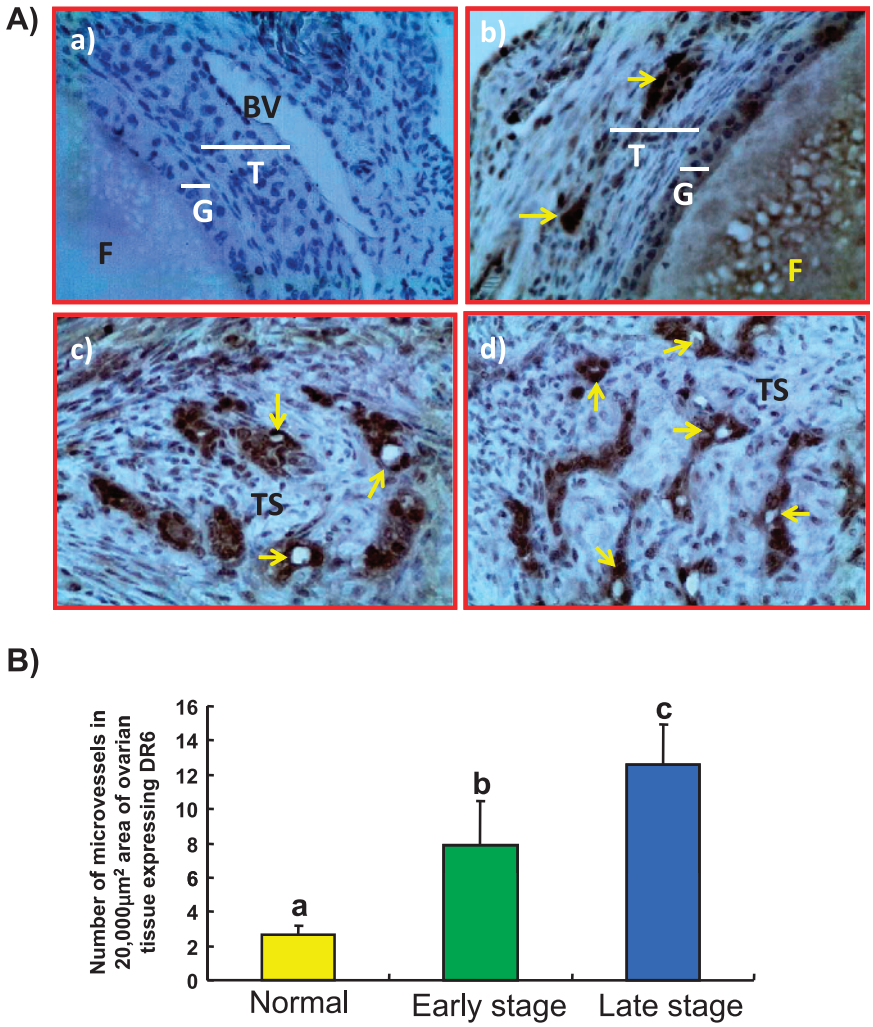

Figure 3. (A) Immunohistochemical detection of DR6-expressing microvessels in hen ovaries with or without tumor. (a) Section of a normal ovarian stroma immunostained by omitting primary antibodies used as control. No immunopositive vessel is seen. (b) Serial section from the same normal ovary immunostained with primary antibodies. Very few DR6-expressing vessels are seen. (c) An ovarian section from a hen with early-stage OVCA. Compared to the normal ovary, many DR6-expressing microvessels are seen in the stroma between tumors. (d) Section of a malignant tumor from a hen with late-stage OVCA. Many DR6-expressing microvessels are localized in the tumor stroma. BV indicates blood vessel; F, follicle; G, granulosa layer; T, theca layer; TS, tumor stroma. Arrows indicate DR6-expressing microvessels. Original magnification, ×40. (B) Changes in the frequency of DR6-expressing ovarian microvessels relative to ovarian tumor development and progression in hens. The frequency of microvessels expressing DR6 in a 20,000-μm^2 area of normal ($n = 15$) and malignant ovaries (expressed as the mean ± SD, $n = 15$ each for early and late stages). Compared to the normal ovary, the frequency of microvessels expressing DR6 was significantly ($P < .001$) higher in hens with early-stage OVCA cancer and increased further ($P < .001$) as the disease progressed to a late stage in hens. Each bar with a different letter indicates significant differences ($P < .001$) between normal and tumor groups.

microvessels in hens with normal ovaries had thick, complete, and continuous vessel walls with intense staining. These vessels were located in the theca layer of the follicles and a few vessels were in the ovarian stroma. In contrast, most of the DR6-expressing vessels in malignant ovaries were discontinuous or incomplete with thin vessel walls (Figure 3*A*). The number of DR6-expressing microvessels was significantly higher ($P < .01$, exact Mann-Whitney test) in hens with early (mean ± SD = 8.0 ± 2.29 microvessels per 20,000-μm^2 area of stroma) and late (13.0 ± 2.37 microvessels per 20,000-μm^2 area of stroma in malignant ovaries) stages of OVCA than in hens with normal ovaries (3.0 ± 0.52 microvessels per 20,000-μm^2 area of stroma in normal ovaries; Figure 3*B*). However, significant differences in the population of DR6-expressing microvessels among the histologic subtypes were not observed.

Tumor cells (Figure 4*A*) as well as a few normal OSE cells expressed DR6. In addition, rounded (T lymphocyte like) to irregularly shaped (macrophage-like) DR6 cells were also detected in the stroma of the normal ovaries or malignant ovaries. Compared with normal ovaries (mean ± SD = $3.6 \times 10^6 \pm 3.8 \times 10^5$ in a 20,000-μm^2 area), the intensities of DR6 staining increased approximately 9-fold ($P < .001$) in hens with early-stage OVCA and 13-fold ($P < .001$) in hens with late-stage OVCA, respectively (Figure 4*B*). However, significant differences in DR6 staining intensities were not observed among three different histologic subtypes of OVCA in hens.

Immunoblot analysis for DR6 protein in ovarian tissues and serum samples. Immunohistochemical expression of DR6 in normal or malignant ovaries was confirmed by immunoblot analysis using homogenates of OSE cells (from normal ovaries) or tumor cells (from malignant ovaries) as well as homogenates from whole normal or malignant ovaries. A band of 50 to 60 kDa was detected in the homogenates of cells (normal OSE cells or tumor cells) and tissues (whole normal or tumor ovaries; Figure 5*A*). In addition, immunoreactive 50- to 60-kDa DR6 protein was also detected by immunoblot analysis in the serum of hens with normal ovaries or those with OVCA (Figure 5*A*). Compared with the whole ovarian homogenates or serum from hens with normal ovaries, immunoreactivity for DR6 protein was intense in the homogenates of malignant ovaries or serum from hens with OVCA (Figure 5*A*). These results support the immunohistochemical observation that OSE in hens with normal ovaries and tumor cells in hens with OVCA express DR6 protein. Moreover, these epithelial cells may be a source of DR6 proteins in the circulation of laying hens because DR6 was detected in the serum of hens with normal ovaries or those with OVCA.

Expression of DR6 messenger RNA. DR6 messenger RNA (mRNA) expression confirmed the observed variations in ovarian DR6 expression among hens with normal ovaries or those with OVCA. Although the patterns of DR6 mRNA expression were similar between normal OSE and tumor cells from early-stage OVCA, it was stronger for tumor cells from late-stage OVCA. Compared with the hens with normal ovaries, strong amplification of signal for DR6 (Figure 5*B*) was observed in the ovarian extracts from hens with early-stage OVCA and the amplification was stronger in hens with late-stage OVCA. However, differences in DR6 mRNA expression were

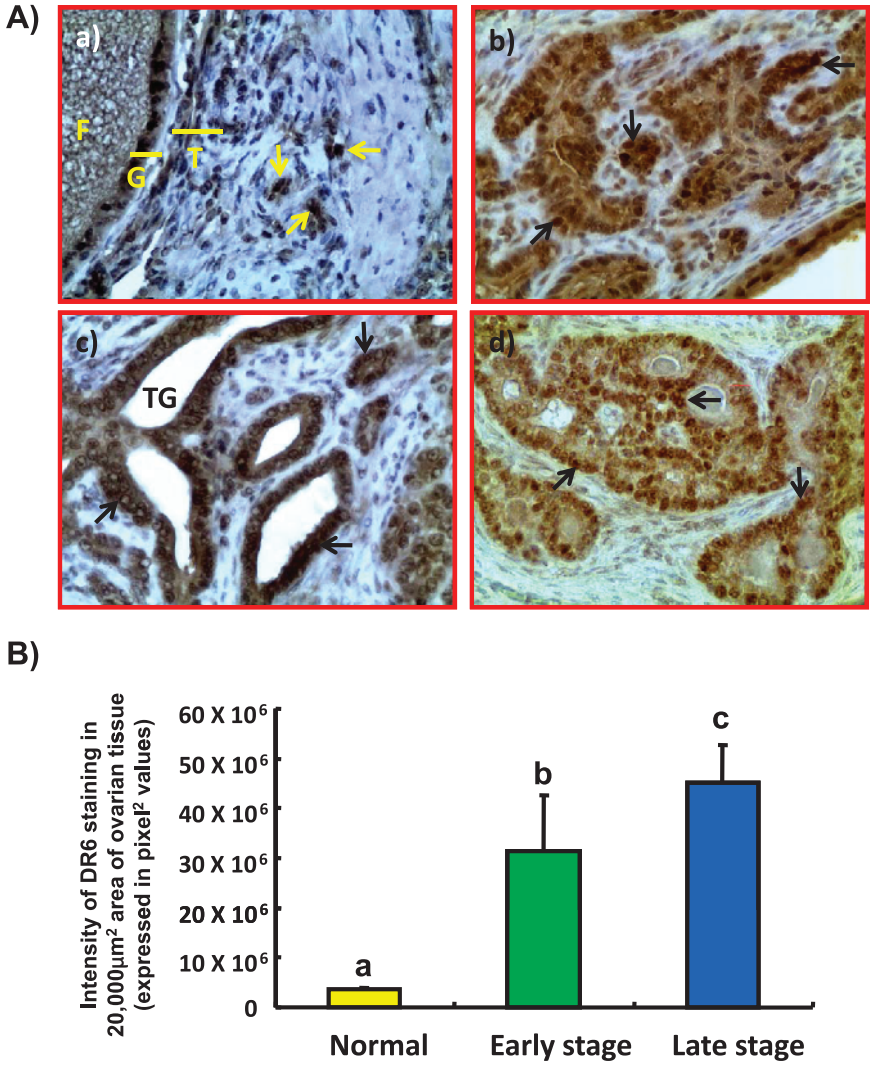

Figure 4. (A) Expression of DR6 by tumor cells in malignant ovaries in hens. (a) Section of a normal ovary immunostained for DR6 expression. Very few immunopositive cells are present in the ovarian stroma. (b-d) Sections of different histologic subtypes of OVCA in hens including serous (b), endometrioid (c), and mucinous (d) at early stages immunostained for DR6 expression. Compared with the normal OSE cells, tumor cells in all three histologic subtypes stained intensely. Original magnification, ×40. (B) Changes in the DR6 staining intensity relative to ovarian tumor development and progression in hens. The intensity of DR6 staining is expressed as the pixel values (mean ± SD) in a 20,000-μm^2 area in normal ovarian stroma ($n = 15$) or in malignant ovaries. Compared to the normal ovary, the intensity of DR6 staining was significantly ($P < .001$) higher in hens with early-stage OVCA ($n = 15$) and increased further ($P < .001$) in late-stage OVCA ($n = 15$). Each bar with different letter indicates significant differences ($P < .001$) among normal or OVCA stages.

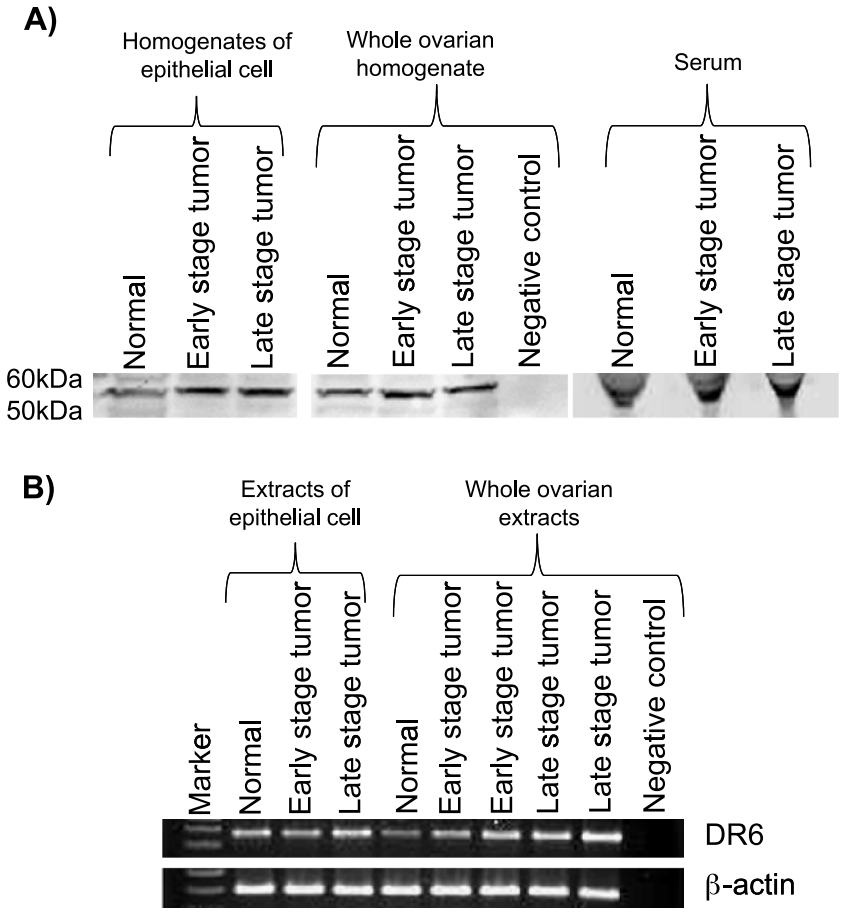

Figure 5. Immunoreactive (A) DR6 protein or (B) mRNA in serum and ovaries of hens with normal ovaries or those with OVCA. (A) One-dimensional Western blot analysis: Immunoreactive DR6 proteins of 50- to 60-kDa molecular weight were detected in the homogenates of normal OSE cells or tumor cells, in homogenates of whole normal or malignant ovaries, as well as in serum of hens by one-dimensional Western blot. Compared to the hens with normal ovaries, relatively stronger immunoreactive bands for DR6 proteins were observed in serum and ovaries of hens with early and late stages of OVCA. No immunoreactive band was detected in the negative control in which protein sample was omitted. (B) Semiquantitative RT-PCR: mRNA expression for DR6 was detected in the extracts of normal OSE cells or tumor cells and in extracts of normal and malignant ovaries by semiquantitative PCR. Compared to the weak expression by normal ovaries and OSE, strong amplification for DR6 mRNA was observed in the extracts of malignant ovaries and tumor cells in hens with early- and late-stage OVCA. No DR6 mRNA expression was detected in the negative control in which mRNA sample was omitted.

not observed among different histologic subtypes of OVCA at the same stage (early or late). Overall, compared to hens with normal ovaries, strong amplification of DR6 mRNA was observed in hens with OVCA as observed for immunoreactivities in immunohistochemistry and immunoblot analysis.

Discussion

This is the first report on the expression of death receptor (DR6) by tumor cells of malignant ovaries in hens. The expression of DR6 was significantly higher in the tumor cells of malignant ovaries than OSE cells of normal ovaries. Furthermore, the population of ovarian microvessels expressing DR6 was significantly higher in hens with early-stage OVCA than hens with normal ovaries and increased further in hens with late-stage OVCA. In addition, DR6 was also detected in the serum of hens. Thus, the results of the present study suggest that the increase in DR6 expression may be associated with ovarian tumor development and progression in laying hens.

Tumor-associated neoangiogenesis (TAN) and suppression of antitumor immunity are two of the early events required for the survival and progression of the tumor. Increased numbers of immature microvessels with disorganized and discontinuous smooth muscle layers are the characteristic features of ovarian TAN in patients as well as in laying hens with OVCA [24]. Compared to hens with normal ovaries, the number of DR6-expressing microvessels was significantly higher in hens with early-stage OVCA and increased further in hens with late-stage OVCA. A recent study has reported increased expression of DR6 by ovarian tumors in patients with advanced-stage OVCA [6]. In this study, the population of DR6-expressing ovarian microvessels increased significantly at an earlier stage even before the tumor became grossly detectable. Recently, DR6 was reported to be required for angiogenesis in the central nervous system [31]. Although precise reason(s) for the increase in the population of DR6-expressing microvessels in malignant ovaries is not known, it is possible that DR6 will play a role in the development of ovarian TAN.

Despite the presence of an antitumor immune response [5,32], the rare eradication of ovarian tumors and their progression suggest that multiple mechanisms are used by the tumor to escape immune rejection. The expression of DR6 has been reported to be increased significantly

in cell lines and patients with prostate and breast cancers [7,10,33]. In the absence of DR6, ligation of the T-cell receptor results in enhanced T-cell proliferation, activation, and skewed T_H2 cytokine production. Similarly, B cells lacking DR6 show increased proliferation, cell division, and cell survival on mitogenic stimulation (anti-CD40 and LPS) or BCR ligation. DR6−/− mice showed increased T_H2 immune responses to both T-dependent and -independent antigens. In contrast, it is suggested that increased DR6 expression on tumor cells results in the cleaving of extracellular part of DR6 from the cell surface by matrix metalloproteinase 14. This shed DR6 reported to attenuate the *in vitro* differentiation of monocytes into immunotolerant instead of immunocompetent dendritic cells, which can contribute to tumor evasion from the immune system [17]. All these reports indicate that DR6 plays important roles in imparting tolerance to local immune response. In the present study, the expression of ovarian DR6 was significantly high in hens with early-stage OVCA than in hens with normal ovaries and increased further in hens with late-stage OVCA. Although the significance of increased DR6 expression by malignant cells is not known, the results of the current study suggest that increased DR6 expression may play important roles in the suppression of immunity against ovarian tumors.

The results of the current study suggest several translational significances. Because the malignant tumors in hens express DR6 and it is also present in the serum, DR6 could be targeted for contrast-enhanced ultrasound imaging to detect the tumor. Thus, use of DR6-expressing epithelium in the ovary as a target may increase the sensitivity of ultrasound scanning to detect OVCA together with serum levels of DR6. Hence, it will bring a significant change in imaging paradigms and improve the specificity of ultrasound scanning. It will also make possible to determine the time between the tumor-associated elevation of DR6 in serum and the earliest detection of tumor by contrast-enhanced ultrasound scanning. This information will enable the detection of OVCA at an early stage and lead to the development of treatment modalities for patients with OVCA. In addition, current findings will also be useful in developing ovarian tumor–associated anti-DR6 therapies, which can be tested in laying hens. Taken together, information on the association of DR6 with the early detection of OVCA and the potential development of anti-DR6–based therapies will establish the foundation for clinical studies. It may thus ultimately lead to the development of an effective diagnostic test and therapies for OVCA at an early stage.

In conclusion, this study showed that the tissue expression of DR6, a potential tumor-associated neoangiogenic and immunosuppressive factor, was significantly higher in hens with early-stage OVCA than in hens with normal ovaries and increased further as the disease progressed to late stages. This information will be useful and contribute to clinical studies to determine the role of DR6 in OVCA development and progression in humans.

Acknowledgments

The authors thank Chet and Pam Utterback and Doug Hilgendorf, staff of the University of Illinois at Urbana-Champaign Poultry Research Farm, for maintenance of the hens. The authors also thank Sergio Abreu Machado and Syed Tahir Abbas Shah, graduate students, Department of Animal Sciences, University of Illinois at Urbana-Champaign, for helping in collecting hen tissue.

References

[1] Jemal A, Siegel R, Xu J, and Ward E (2010). Cancer statistics, 2010. *CA Cancer J Clin* **60**, 277–300.

[2] Ferlay J, Autier P, Boniol M, Heanue M, Colombet M, and Boyle P (2007). Estimates of the cancer incidence and mortality in Europe in 2006. *Ann Oncol* **18**, 581–592.

[3] Liu VC, Wong LY, Jang T, Shah AH, Park I, Yang X, Zhang Q, Lonning S, Teicher BA, and Lee C (2007). Tumor evasion of the immune system by converting $CD4^+CD25^-$ T cells into $CD4^+CD25^+$ T regulatory cells: role of tumor-derived TGF-β. *J Immunol* **178**, 2883–2892.

[4] Curiel TJ (2007). Tregs and rethinking cancer immunotherapy. *J Clin Invest* **117**, 1167–1174.

[5] Yigit R, Massuger LF, Figdor CG, and Torensma R (2010). Ovarian cancer creates a suppressive microenvironment to escape immune elimination. *Gynecol Oncol* **117**, 366–372.

[6] Sasaroli D, Gimotty PA, Pathak HB, Hammond R, Kougioumtzidou E, Katsaros D, Buckanovich R, Devarajan K, Sandaltzopoulos R, Godwin AK, et al. (2011). Novel surface targets and serum biomarkers from the ovarian cancer vasculature. *Cancer Biol Ther* **12**, 169–180.

[7] Benschop R, Wei T, and Na S (2009). Tumor necrosis factor receptor superfamily member 21: TNFR-related death receptor 6, DR6. In *Therapeutic Targets of the TNF Superfamily.* IS Grewal (Ed). Landes Bioscience, Austin, TX. Available at: http://www.landesbioscience.com/books/1137/.

[8] Locksley RM, Killeen N, and Lenardo MJ (2001). The TNF and TNF receptor superfamilies: integrating mammalian biology. *Cell* **104**, 487–501.

[9] Pan G, Bauer JH, Haridas V, Wang S, Liu D, Yu G, Vincenz C, Aggarwal BB, Ni J, and Dixit VM (1998). Identification and functional characterization of DR6, a novel death domain-containing TNF receptor. *FEBS Lett* **431**, 351–356.

[10] Kasof GM, Lu JJ, Liu D, Speer B, Mongan KN, Gomes BC, and Lorenzi MV (2001). Tumor necrosis factor-alpha induces the expression of DR6, a member of the TNF receptor family, through activation of NF-κB. *Oncogene* **20**, 7965–7975.

[11] Buckanovich RJ, Sasaroli D, O'Brien-Jenkins A, Botbyl J, Hammond R, Katsaros D, Sandaltzopoulos R, Liotta LA, Gimotty PA, and Coukos G (2007). Tumor vascular proteins as biomarkers in ovarian cancer. *J Clin Oncol* **25**, 852–861.

[12] Wick M, Dubey P, Koeppen H, Siegel CT, Fields PE, Chen L, Bluestone JA, and Schreiber H (1997). Antigenic cancer cells grow progressively in immune hosts without evidence for T cell exhaustion or systemic anergy. *J Exp Med* **186**, 229–238.

[13] Gajewski TF, Meng Y, and Harlin H (2006). Immune suppression in the tumor microenvironment. *J Immunother* **29**, 233–240.

[14] Clarke B, Tinker AV, Lee CH, Subramanian S, van de Rijn M, Turbin D, Kalloger S, Han G, Ceballos K, Cadungog MG, et al. (2009). Intraepithelial T cells and prognosis in ovarian carcinoma: novel associations with stage, tumor type, and BRCA1 loss. *Mod Pathol* **22**, 393–402.

[15] Zhang L, Conejo-Garcia JR, Katsaros D, Gimotty PA, Massobrio M, Regnani G, Makrigiannakis A, Gray H, Schlienger K, Liebman MN, et al. (2003). Intratumoral T cells, recurrence, and survival in epithelial ovarian cancer. *N Engl J Med* **348**, 203–213.

[16] Barua A, Bradaric MJ, Kebede T, Espionosa S, Edassery SL, Bitterman P, Rotmensch J, and Luborsky JL (2007). Anti-tumor and anti-ovarian autoantibodies in women with ovarian cancer. *Am J Reprod Immunol* **57**, 243–249.

[17] DeRosa DC, Ryan PJ, Okragly A, Witcher DR, and Benschop RJ (2008). Tumor-derived death receptor 6 modulates dendritic cell development. *Cancer Immunol Immunother* **57**, 777–787.

[18] Steinman RM and Nussenzweig MC (2002). Avoiding horror autotoxicus: the importance of dendritic cells in peripheral T cell tolerance. *Proc Natl Acad Sci USA* **99**, 351–358.

[19] Barua A, Bitterman P, Abramowicz JS, Dirks AL, Bahr JM, Hales DB, Bradaric MJ, Edassery SL, Rotmensch J, and Luborsky JL (2009). Histopathology of ovarian tumors in laying hens: a preclinical model of human ovarian cancer. *Int J Gynecol Cancer* **19**, 531–539.

[20] Rodriguez-Burford C, Barnes MN, Berry W, Partridge EE, and Grizzle WE (2001). Immunohistochemical expression of molecular markers in an avian model: a potential model for preclinical evaluation of agents for ovarian cancer chemoprevention. *Gynecol Oncol* **81**, 373–379.

[21] Giles JR, Elkin RG, Trevino LS, Urick ME, Ramachandran R, and Johnson PA (2010). The restricted ovulator chicken: a unique animal model for investigating the etiology of ovarian cancer. *Int J Gynecol Cancer* **20**, 738–744.

[22] Bridgham JT, Bobe J, Goetz FW, and Johnson AL (2001). Conservation of death receptor-6 in avian and piscine vertebrates. *Biochem Biophys Res Commun* **284**, 1109–1115.

[23] Barua A, Abramowicz JS, Bahr JM, Bitterman P, Dirks A, Holub KA, Sheiner E, Bradaric MJ, Edassery SL, and Luborsky JL (2007). Detection of ovarian tumors

in chicken by sonography: a step toward early diagnosis in humans? *J Ultrasound Med* **26**, 909–919.

[24] Barua A, Bitterman P, Bahr JM, Bradaric MJ, Hales DB, Luborsky JL, and Abramowicz JS (2010). Detection of tumor-associated neoangiogenesis by Doppler ultrasonography during early-stage ovarian cancer in laying hens: a preclinical model of human spontaneous ovarian cancer. *J Ultrasound Med* **29**, 173–182.

[25] Giles JR, Olson LM, and Johnson PA (2006). Characterization of ovarian surface epithelial cells from the hen: a unique model for ovarian cancer. *Exp Biol Med (Maywood)* **231**, 1718–1725.

[26] Yellapa A, Bahr JM, Bitterman P, Abramowicz JS, Edassery SL, Penumatsa K, Basu S, Rotmensch J, and Barua A (2012). Association of interleukin 16 with the development of ovarian tumor and tumor-associated neoangiogenesis in laying hen model of spontaneous ovarian cancer. *Int J Gynecol Cancer* **22**, 199–207.

[27] Barua A, Edassery SL, Bitterman P, Abramowicz JS, Dirks AL, Bahr JM, Hales DB, Bradaric MJ, and Luborsky JL (2009). Prevalence of antitumor antibodies in laying hen model of human ovarian cancer. *Int J Gynecol Cancer* **19**, 500–507.

[28] Khan M, Bahr JM, Yellapa Y, Bitterman P, Abramowicz JS, Edassery SL, Basu S, Rotmensch J, and Barua B (2012). Association of immunoglobulin like transcript 3 (ILT3) with the progression of ovarian tumors in laying hens, a preclinical model of spontaneous ovarian cancer. *Transl Oncol* **5**, 85–91.

[29] Barua A, Bitterman P, Bahr JM, Basu S, Sheiner E, Bradaric MJ, Hales DB, Luborsky JL, and Abramowicz JS (2011). Contrast-enhanced sonography depicts spontaneous ovarian cancer at early stages in a preclinical animal model. *J Ultrasound Med* **30**, 333–345.

[30] Hong YH, Lillehoj HS, Lee SH, Dalloul RA, and Lillehoj EP (2006). Analysis of chicken cytokine and chemokine gene expression following *Eimeria acervulina* and *Eimeria tenella* infections. *Vet Immunol Immunopathol* **114**, 209–223.

[31] Tam SJ, Richmond DL, Kaminker JS, Modrusan Z, Martin-McNulty B, Cao TC, Weimer RM, Carano RA, van Bruggen N, and Watts RJ (2012). Death receptors DR6 and TROY regulate brain vascular development. *Dev Cell* **22**, 403–417.

[32] Kandalaft LE, Singh N, Liao JB, Facciabene A, Berek JS, Powell DJ Jr, and Coukos G (2010). The emergence of immunomodulation: combinatorial immunochemotherapy opportunities for the next decade. *Gynecol Oncol* **116**, 222–233.

[33] Klima M, Zajedova J, Doubravska L, and Andera L (2009). Functional analysis of the posttranslational modifications of the death receptor 6. *Biochim Biophys Acta* **1793**, 1579–1587.

Translational Oncology
www.transonc.com

Volume 5 Number 2 April 2012 pp. 85–91 85

Expression of Leukocyte Inhibitory Immunoglobulin-like Transcript 3 Receptors by Ovarian Tumors in Laying Hen Model of Spontaneous Ovarian Cancer[1]

Mohammad Faisal Khan*, Janice M. Bahr†, Aparna Yellapa*, Pincas Bitterman‡, Jacques S. Abramowicz§, Seby L. Edassery*, Sanjib Basu¶, Jacob Rotmensch§ and Animesh Barua*,‡,§

*Department of Pharmacology, Rush University Medical Center, Chicago, IL, USA; †Department of Animal Sciences, University of Illinois at Urbana-Champaign, Champaign, IL, USA; ‡Department of Pathology, Rush University Medical Center, Chicago, IL, USA; §Department of Obstetrics and Gynecology, Rush University Medical Center, Chicago, IL, USA; ¶Department of Preventive Medicine (Biostatistics), Rush University Medical Center, Chicago, IL, USA

Abstract

Attempts to enhance a patient's immune response and ameliorate the poor prognosis of ovarian cancer (OVCA) have largely been unsuccessful owing to the suppressive tumor microenvironment. Leukocyte immunoglobulin-like transcript 3 (ILT3) inhibitory receptors have been implicated in immunosuppression in several malignancies. The expression and role of ILT3 in the progression of ovarian tumors are unknown. This study examined the expression and association of ILT3 in ovarian tumors in laying hens, a spontaneous preclinical model of human OVCA. White Leghorn laying hens were selected by transvaginal ultrasound scanning. Serum and normal ovaries or ovarian tumors were collected. The presence of tumors and the expression of ILT3 were examined by routine histology, immunohistochemistry, Western blot analysis, and reverse transcription–polymerase chain reaction. In addition to stromal immune cell-like cells, the epithelium of the ovarian tumors also expressed ILT3 with significantly high intensity than normal ovaries. Among different subtypes of ovarian carcinomas, serous OVCA showed the highest ILT3 staining intensity, whereas endometrioid OVCA had the lowest intensity. Similar to humans, an immunoreactive protein band of approximately 55 kDa for ILT3 was detected in the ovarian tumors in hens. The patterns of ILT3 protein and messenger RNA expression by ovarian tumors in different subtypes and stages were similar to those of immunohistochemical staining. The results of this study suggest that laying hens may be useful to generate information on ILT3-associated immunosuppression in OVCA. This animal model also offers the opportunity to develop and test anti-ILT3 immunotherapy to enhance antitumor immunity against OVCA in humans.

Translational Oncology (2012) 5, 85–91

Introduction

Despite the remarkable improvements in cytoreductive surgeries and chemotherapeutics, ovarian cancer (OVCA) remains one of the most lethal gynecologic malignancies of women with a high death rate [1]. Owing to the lack of an effective early detection test, OVCA in most cases is detected at late stages, and its high recurrence rate (80%-90%) contributes to poor prognosis [2,3]. There is an emerging recognition that tumor growth, in general, elicits specific immune responses mediated by cell-mediated immunity [4]. As a result, immunotherapies against several cancers are being developed [4–6]. Although recent

Address all correspondence to: Animesh Barua, PhD, Laboratory for Translational Research on Ovarian Cancer, Department of Pharmacology, Room # 410, Cohn Building, Rush University Medical Center, 1735 W Harrison St, Chicago, IL 60612.
E-mail: Animesh_Barua@rush.edu

[1]This study was supported by the Idea Development Award from the United States Department of Defense (OCno. 093303), National Cancer Institute Pacific Ovarian Cancer Research Consortium Career Development Program grant P50 CA83636, and the Elmer Sylvia and Sramek Foundation (USA). The authors declare no conflict of interest.
Received 16 November 2011; Revised 23 December 2011; Accepted 3 January 2012

DOI 10.1593/tlo.11328

advances in immunotherapy have been shown to improve the overall survival ability of patients with hematologic tumors and melanoma [7], most immunotherapeutic trials have failed to demonstrate success in clinical responses [6,8]. Thus, development of new strategies to promote immune responses against malignancies is critical in overcoming the limited efficacy of conventional therapies. Despite the presentation of antigens by ovarian malignant cells, which should induce immune-mediated rejection, spontaneous rejection of an established tumor is rare [9]. This lack of immune response is not only because of the ignorance of the immune system but also because of the tumor-induced immune suppression that protects the tumor from eradication [9]. Therefore, a better understanding of the mechanisms of tumor-induced immunosuppression will enhance our ability to prevent ovarian tumor progression and to design antitumor interventional strategies.

Numerous studies on cancers of several organs have reported several mechanisms of tumor-induced immune suppression including induction of regulatory T cells [10], expression of immunosuppressive factors (transforming growth factor β, interleukin 10, and chemokine ligand 22) [10–12], down-regulation of intracellular adhesion molecules [13], and induction of peripheral tolerance [4,14,15]. In contrast, studies on the mechanism of immune suppression in ovarian malignancy are very limited. OVCA differs from other malignancies in its specific dissemination pattern [9]. The tumor typically spreads in a diffuse intra-abdominal fashion rather than through systemic circulation. Thus, antitumor immune response at the tumor environment plays a critical role to ovarian tumor metastasis. Immunosuppressive regulatory T cells [10], transforming growth factor β [11,12], tolerance-inducing plasmacytoid dendritic cells [16], B7-H4+ macrophages [17], and interleukin 10 [18] have been reported to be present in the tumor microenvironment. However, how these immunosuppressive factors and agents are recruited into the tumor environment is not known. Emerging studies suggest that induction of inhibitory receptor immunoglobulin (Ig)-like transcript 3 (ILT3) expression is one of the mechanisms contributing to the tumor-induced immune suppression in several malignancies [19].

ILT3 is a member of leukocyte Ig-like receptors family with inhibitory functions and exists in both membrane and soluble forms [20]. Both forms of ILT3s have been suggested to inhibit T-cell proliferation, $CD4^+$ T-cell anergy, suppressing the differentiation of interferon γ–producing $CD8^+$ cytotoxic lymphocytes. In addition, membrane and soluble ILT3 were also reported to stimulate the differentiation of regulatory T cells in various cancer patients [4,5,10]. All these findings suggest that ILT3 may be involved in the immunosuppression against tumor antigens and prevention or blocking of ILT3 expression may enhance a patient's immune responses to malignancies. The expression of ILT3 in OVCA patients has not yet been reported. Difficulties in identifying and access to patients at the early stage of OVCA hinder the ability to study the involvement of ILT3 in OVCA progression and develop interventional strategies for its prevention. Rodents do not develop OVCA spontaneously, and the histopathologies of induced OVCA in rodents do not resemble the spontaneous OVCA in humans [21]. Recently, we have shown that laying hens are the only widely available animals that develop OVCA spontaneously with a high incidence rate and histopathologies remarkably similar to human OVCA [22]. The expression of leukocyte Ig-like receptors has been reported in chicken, which are shown to be orthologus to those of mammals including humans [23,24]. Thus, the goal of this study was to examine whether ILT3 is expressed in ovarian tumors in the laying hen model of spontaneous OVCA and, if so, whether ILT3 expression is associated with the progression of ovarian tumors in hens.

Materials and Methods

Animals

Commercial strains of approximately 3-year-old white Leghorn laying hens (*Gallus domesticus*) were selected from a flock of layers maintained under standard poultry husbandry practices. The incidence of OVCA in hens of this age group is approximately 15% to 20% and is associated with low or complete cessation of egg laying [25]. Hens (n = 148) were selected on the basis of their egg-laying rates (normal, low, or ceased egg laying) and transvaginal ultrasound scanning as reported previously [25]. All experimental procedures were performed according to the institutional animal care and use committee approved protocol.

Tissue Collection and Processing

Serum samples. Blood was obtained from brachial veins of all hens before euthanasia, centrifuged (1000g for 20 minutes), and serum samples were stored at −80°C until further use.

Gross ovarian morphology and histopathology. Ovarian pathology and tumor staging were performed by gross and histologic examination as reported previously [22]. Each normal ovary or ovary with tumor was divided into four portions for protein extraction, total RNA collection, paraffin and frozen embedding for routine histology, and immunohistochemical studies as reported previously [26]. Ovarian surface epithelial (OSE) cells from normal or ovaries with tumor were collected similarly as reported earlier [27]. All collected samples were grouped into three groups including normal-, early-, and late-stage OVCA based on the diagnosis of the histopathologic ovarian tissue examination as reported previously [22].

Preparation of Ovarian Specimen for Biochemical Analysis

Snap-frozen normal ovaries and ovaries with tumor as well as OSE from normal ovaries and ovaries with tumor were homogenized with a Polytron homogenizer (Brinkman Instruments, Westbury, NY) as reported previously [28] and centrifuged, the supernatant was collected, and the protein content of the extract was measured and stored at −80°C until further use.

Histopathologic Examination and Immunohistochemistry

Paraffin or frozen sections from each ovary with tumor or ovaries that appeared normal without any grossly detectable tumor were stained with hematoxylin and eosin and observed under a light microscope. Presence or absence of tumors in the section and their histologic types were determined as reported earlier [22]. Immunohistochemical detection of ILT3 expression was performed using goat anti-ILT3 (R&D Systems, Inc, Minneapolis, MN) as primary antibodies (n = 15 hens each, for normal, early, and late stages as reported previously) [26]. The number of hens for each group was determined based on statistical power analysis to achieve significant differences in the intensities of ILT3 immunostaining among the hens of normal or OVCA groups. These hens were selected from each group randomly. Briefly, sections were deparaffinized, and antigens on the sections were unmasked by heating the sections with an antigen-unmasking solution (Vector Laboratories, Burlingame, CA) for 20 minutes in a microwave oven. Endogenous peroxidase in the

sections was inactivated, and nonspecific staining was blocked by incubating with 0.3% hydrogen peroxide in methanol for 30 minutes followed by 1% (vol/vol) normal horse serum for 15 minutes, respectively. Sections were then incubated overnight with primary antibodies (1:100 dilution) followed by 1 hour of incubation with anti-goat IgG-HRP secondary antibodies (R&D Systems). Immunoprecipitates on the sections were visualized by incubation with a mixture of diaminobenzidine and hydrogen peroxide in diaminobenzidine buffer (Vector Laboratories). Sections were then counterstained with hematoxylin, dehydrated, and covered. Control staining was carried out simultaneously in which the first antibodies were omitted and normal goat serum was used. No staining was found in these control slides.

Sections were then examined under a light microscope attached to digital imaging software (MicroSuite version 5; Olympus Corporation, Tokyo, Japan). Three sections per ovary and five regions of interest (20,000 μm^2/region at ×40 objective and ×10 ocular magnification) per section were randomly selected. Using the software, the intensity of the ILT3 immunostaining in each region was measured and recorded as pixel values in 20,000 μm^2 of the section. The mean of pixel values of these five regions in a section was considered as the intensity of each section, and the mean of intensities of three sections was considered as the mean of ILT3 staining intensity in normal or tumor-bearing ovaries.

One-dimensional Western Blot

The expression of ILT3 proteins by normal ovaries or ovarian tumors as well as OSE from normal ovaries or ovaries with tumor was determined by Western blot analysis using primary and secondary antibodies mentioned above. On the basis of immunohistochemical staining results, representative samples of ovarian as well as OSE homogenates from normal or ovarian tumors at early and late stages were used in immunoblot analysis. Immunoreactions on the membrane were visualized as a chemiluminescence product (Super Dura West substrate; Pierce/Thermo Fisher, Rockford, IL), and the image was captured using a Chemidoc XRS (Bio-Rad, Hercules, CA). Digital images obtained with Chemidoc XRS were analyzed by Quantity One software (Bio-Rad) according to the manufacturer's recommendation, and the intensities of immunoreactive bands were expressed as density per intensity in squared millimeter and the mean of intensities for each normal or pathologic group as well as for the stages of OVCA were calculated. No immune reaction was observed in controls where protein samples were omitted. Serum samples for Western blot analysis were selected similar to ovarian samples and tested to confirm the presence of soluble ILT3.

Reverse Transcription–Polymerase Chain Reaction

ILT3 messenger RNA (mRNA) expression in ovarian tissues or epithelial cells from normal hens or hens with OVCA was assessed by semiquantitative reverse transcription–polymerase chain reaction (RT-PCR) as reported previously [29]. Representative samples of normal ovaries or ovaries with tumor as well as OSE from hens were selected for RT-PCR analyses based on their immunoreactivities in immunohistochemistry and immunoblot analysis were used. Hen-specific ILT3 primers were designed by Oligoperfect Designer software (Invitrogen, Carlsbad, CA) using the ILT3 sequence from the National Center for Biotechnology Information (GenBank: NM_001146134.1). The forward primer was 5-TGG CTG TAC CAG GAA AGA GG and the reverse primer was 5-CTC TGA TGC CCC TAC TGA CC. β-Actin was used as the endogenous control with a forward primer of TGCGTGACATCAAGGAGAAG and a reverse primer of ATGCCAGGGTACATTGTGGT. The expected base pair size for the ILT3 amplicon was 150 bp and that for β-actin was 300 bp. PCR amplicons were visualized in a 3% agarose gel (Pierce) in TAE buffer and stained with ethidium bromide, and images were captured using a ChemiDoc XRS system (Bio-Rad). PCR products were sequenced, and the sequence was the same as the sequence of primers from the National Center for Biotechnology Information GenBank (NM_001146134.1).

Statistical Analysis

The differences in the pixel intensities of ILT3 immunostaining among different histologic subtypes and stages (early *vs* late) were assessed by two-way analysis of variance. This was followed by pairwise comparison between the histologic subtypes (normal, endometrioid, mucinous, and serous) within each stage and comparison of the stages within histologic subtypes by two-sample *t* tests and alternative Mann-Whitney tests. All reported *P* values are 2-sided, and $P < .05$ was considered significant. Statistical analyses were performed with SPSS (PASW) version 18 software (IBM, Inc, Armonk, NY) and R statistical software.

Results

Morphologic and Histologic Features of Hen Ovaries and Ovarian Tumors

Gross morphology. A fully functional ovary in a healthy laying hen contained five to six developing large preovulatory follicles (Figure 1*A*), whereas the ovaries of low-laying healthy hens contained less than three preovulatory follicles. In normal hens that had stopped egg laying, ovaries and oviducts were regressed without any detectable abnormality. Solid tissue masses either limited to a small part or to the whole ovary and with or without ascites were observed in 14 hens and

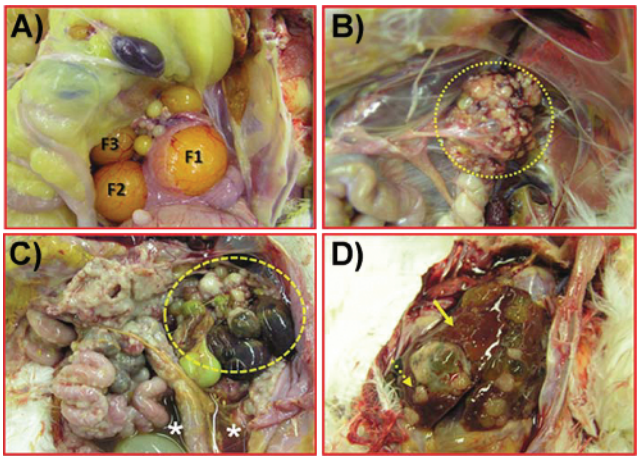

Figure 1. Gross morphology of normal ovaries and ovaries with tumor in laying hens. (A) Normal ovary: A normal laying hen ovary contained a hierarchy of multiple large preovulatory follicles (F1-F3) with an active oviduct. (B) OVCA at early stage in a laying hen. The tumor mass was limited to the ovary (shown in a dotted circle). (C and D) OVCAs at late stages in laying hens. Tumors were metastasized to distant organs including intestine (C) and liver (D, arrows indicate the examples of tumor seeding) with accompanied profuse ascites (*).

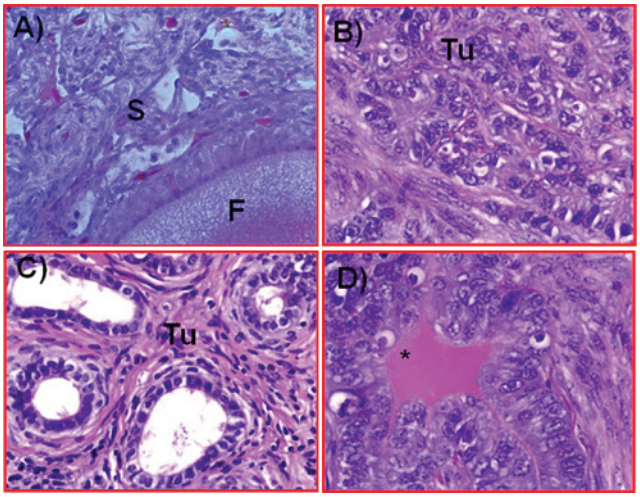

Figure 2. Histologic presentation of different types of malignant ovarian tumors in laying hens detected in the present study. Formalin-fixed paraffin-embedded ovarian tissues were stained for hematoxylin and eosin. (A) A section of a normal ovary showing a follicle embedded in the ovarian stroma. (B) A section of an ovarian serous carcinoma-containing tumor cells with large pleomorphic nucleus and mitotic nuclear bodies. (C) A section of an ovarian endometrioid carcinoma showing confluent back-to-back tumor glands containing a single layer of epithelium with sharp luminal margin. (D) A section of an ovarian mucinous carcinoma. The tumor contained a single layer of columnar epithelium with intercalated ciliated goblet cells. Mucin-like secretion is seen in the lumen of the tumor gland (*). Original magnifications: ×40. F indicates follicle; S, stroma; Tu, tumor.

classified as hens with early-stage OVCA (Figure 1*B*). In 17 hens, the tumor had metastasized to abdominal organs with moderate to profuse ascites and classified as hens with late-stage OVCA (Figure 1, *C* and *D*).

Histopathology. A total of 105 hens were found to have normal ovaries in which embedded primordial and primary follicles were observed in the ovarian stromal tissue (Figure 2*A*). Ovarian tumors were confirmed by routine histology in 31 hens that had solid masses limited to the ovaries (n = 14, early stage) or metastasized to other organs (n = 17, late stage). In addition, microscopic OVCAs were detected in 12 hens without any grossly detectable solid mass in the ovary and grouped in early-stage OVCA. Thus, a total of 26 (14 + 12) hens had early and 17 had late-stage OVCA. Tumors were typed (Figure 2, *B-D*) as serous (n = 18), endometrioid (n = 13), mucinous (n = 10), as well as mixed (n = 2, seromucinous and endoserous) as reported previously [22].

Tissue Expression of ILT3

Immunohistochemical detection of ovarian ILT3 expression. T-lymphocyte-like rounded cells and macrophage-like irregular-shaped cells in the stroma of normal ovaries or ovaries with tumor were found positive for ILT3. Some surface epithelial cells (not all) above the developing cortical follicles in normal ovaries and the epithelium of the ovarian tumors were also stained positive for ILT3 expression (Figure 3, *A-D*). The expression of ILT3 by the epithelial cells of the tumor in hens with OVCA varied with respect to the histologic subtypes of tumors and their stages. As compared with normal hens (mean ± SD = 23029.23 ± 2725.01), the intensities of ILT3 expression were significantly higher (P < .001) in hens with early-stage OVCA irrespective of their histologic subtypes (Figure 4). Similar patterns were also observed for hens with late-stage OVCA.

Among different histologic subtypes at early-stage OVCA, the intensities of ILT3 staining were lowest in hens with ovarian endometrioid tumors (mean ± SD = 36,807.56 ± 2843.56) followed by mucinous (40,207.86 ± 2858.27) and highest in serous OVCA (40,924.40 ± 1400.26) in a 20,000-μm^2 area of tissue (Figure 4). The differences in ILT3 staining intensities were significantly higher in hens with serous OVCA than hens with endometrioid OVCA irrespective of their stages (P < .028 and .025 for early and late stages of OVCA, respectively). However, significant differences in ILT3 staining intensities were not observed between the hens with ovarian endometrioid and mucinous OVCA as well as mucinous and serous OVCA at early and late stages. In hens with serous OVCA, the intensities of ILT3 staining were significantly high in late stages than in early stage (P < .05). However, a significant difference in ILT3 staining intensities between the early and late stages of hens with ovarian endometrioid or mucinous OVCA was not observed.

Immunoblot analysis for ILT3 protein in ovarian tissues and serum samples. Immunohistochemical observation of ILT3 expression was confirmed by immunoblot analysis using homogenates of normal ovaries and ovaries with tumors as well as OSE from normal ovaries and ovarian tumors. As expected, immunoreactive ILT3 protein with a band size of approximately 55 kDa was detected in the homogenates of OSE and ovarian tissues from normal hens and hens with OVCA at early stage (Figure 5*A*). Similar patterns were also observed for serum

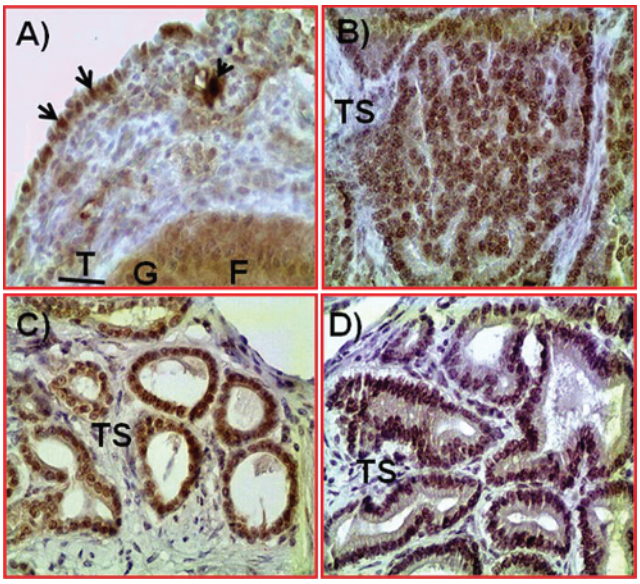

Figure 3. Expression of ILT3 by normal ovaries or ovaries with tumor in laying hens. (A) A section of normal ovary showing ILT3+ OSE cells (examples are shown by arrows) near a developing follicle. An immune cell-like ILT3+ cell is seen beneath the ovarian surface (arrowhead). (B-D) Expression of ILT3 by the epithelium of the ovarian serous (B), endometrioid (C), and mucinous (D) carcinomas at late stages in laying hens. Intense staining for ILT3 by epithelial cells of the tumors was observed in all tumor types. F indicates follicle; G, granulosa layer; T, theca layer; TS, tumor stroma.

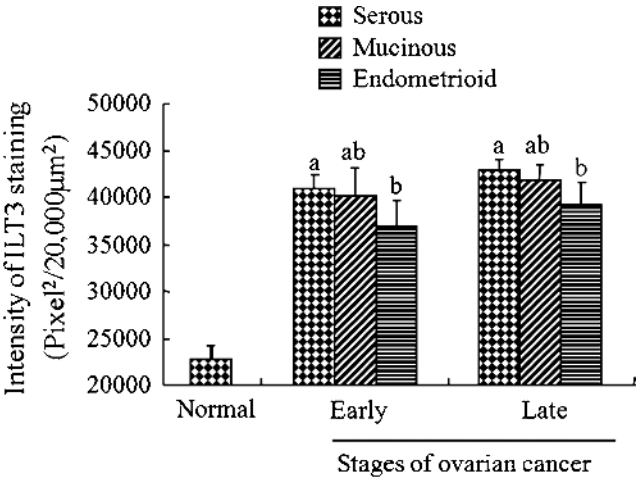

Figure 4. Changes in the ovarian ILT3 expression are associated with ovarian tumor development and progression. The intensity of ILT3 staining is expressed as pixel values (mean ± SD) in a 20,000-μm^2 area of the ovarian stroma in normal ovaries or ovaries with tumor. Compared with normal hens, the intensities of the ILT3 staining were significantly greater in hens with early-stage OVCA ($P < .001$) and increased further in hens with late-stage OVCA irrespective of their tumor types. The intensity of ILT3 staining was significantly lower ($P < .03$) in hens with endometrioid OVCA than hens with serous OVCA. Significant differences were not observed in the intensity of ILT3 staining between the hens with serous and mucinous OVCA irrespective of their stages. Bars with different letters within the same group indicate significant differences in ILT3 staining intensity.

samples (data not shown). Compared with the normal OSE or OSE from ovarian tumors at early stage, ILT3 protein expression was stronger in the OSE from hens at late-stage OVCA (Figure 5*A*). Conversely, the expression of immunoreactive ILT3 proteins was weaker in the homogenates of ovarian endometrioid tumors, moderate in mucinous, and stronger in ovarian serous tumors at the early stage (Figure 5*A*). Similar patterns were also observed for ovarian tumors at late stage (data not shown). These results confirm the immunohistochemical observation that epithelial cells of ovarian tumors in hens express ILT3.

Expression of ILT3 mRNA. Observed variations in ILT3 protein expression among different histologic subtypes of OVCA and their stages were confirmed by ILT3 mRNA expression. Hens with early serous and mucinous ovarian tumors showed strong amplification signal for ILT3, whereas its amplification was low for endometrioid ovarian tumors. However, no differences were observed for ILT3 mRNA expression by different histologic subtypes of late-stage OVCA (Figure 5*B*). Similar patterns were also observed for the epithelial cells of ovarian tumors. Thus, the results of gene expression study confirm the immunohistochemical and immunoblot analysis observations that the epithelium of ovarian tumors expresses ILT3 proteins.

Discussion

This is the first report on the expression of ILT3 by the epithelium of ovarian tumors in laying hens, an animal model of spontaneous OVCA. This study showed that the expression of ILT3 increases significantly in association with ovarian tumor development and progression. These results suggest that laying hens can be used to generate information on the mechanism of spontaneous ovarian tumor–associated immunosuppression and may lead to the development of antitumor immunotherapies and the testing of their efficacies.

Recent progresses in the understanding of tumor-immune interactions have led to the successful development of a number of immunotherapeutic approaches. However, tumor escape from immune recognition is a significant barrier to the success of these immunotherapies. Although the process of escaping immune surveillance by tumors or suppression of antitumor immune response is not well understood, tumor cells, immune cells, and other stromal cells in the tumor surroundings have been reported to interact and create an immunosuppressive microenvironment through a variety of immunosuppressive factors [30]. Enhanced expression of ILT3 by few members of the immune system has been suggested as one of such immunosuppressive factors in the tumor microenvironment [31]. In the present study, in addition to immune cell-like cells, the epithelium of the ovarian tumors in laying hens also

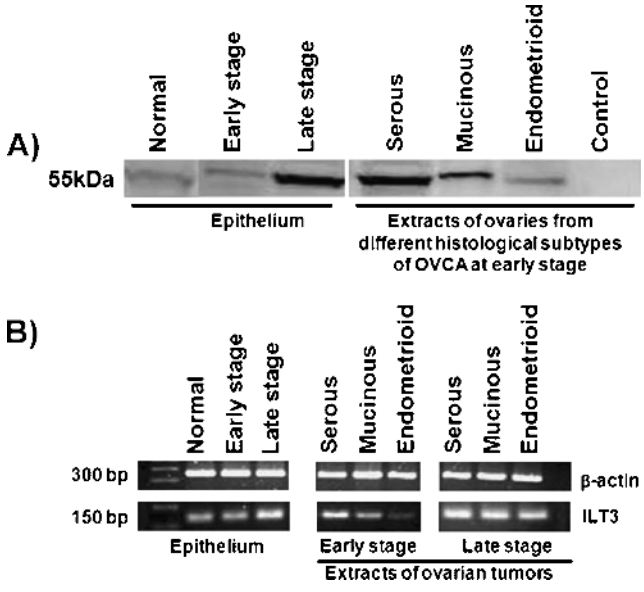

Figure 5. Examples of immunoreactive ILT3 protein (A) or mRNA (B) expression in the homogenates of OSE and ovaries from normal hens or hens with OVCA by one-dimensional Western blot (WB) analysis and semiquantitative PCR, respectively. One-dimensional WB (A): Immunoreactive ILT3 protein of approximately 55-kDa molecular weight was detected in the 1) OSE extract from normal or ovarian tumors and 2) homogenates from different histologic subtypes of ovarian tumors at early stage of OVCA. Compared with the normal OSE or OSE from ovarian tumors at early stage, ILT3 protein expression was stronger in the OSE from hens at late-stage OVCA. Serous ovarian tumors at the early stage showed strong ILT3 staining followed by mucinous and endometrioid tumors. No ILT3 expression was detected in negative control in which protein sample was omitted. RT-PCR (B): mRNA expression by the OSE extract from normal or ovarian tumor and from different histologic subtypes of ovarian tumors at early and late stages of OVCA. Compared to the normal OSE, or OSE from ovarian tumor at early stage, a strong expression of ILT3 mRNA was observed in the OSE from hens with late-stage OVCA. Similarly, strong expression patterns were also observed for the homogenates of ovarian tumors at late stages than early stages irrespective of tumor subtypes. As observed in immunohistochemistry and immunoblot analysis, endometrioid tumors at early stage were weaker in ILT3 mRNA expression than their counterpart serous and mucinous tumors. No ILT3 mRNA expression was detected in the negative control in which mRNA sample was omitted.

expressed ILT3. Under normal physiological condition, ILT3 has been reported to be expressed selectively by professional antigen-presenting cells including monocytes, macrophages, and dendritic cells [32]. The expression of ILT3 on exposure to alloantigen-specific suppressor T cells or cytokines by nonprofessional antigen-presenting cells, like endothelial cells as well as tumor cells from chronic lymphocytic leukemia, was also reported previously [33,34]. Thus, the present results suggest that ovarian tumors also express immunosuppressive ILT3 as reported for few other cancers.

In the present study, compared with normal hens, the intensity of the ILT3 expression was significantly high in hens with early-stage OVCA and increased further as the disease progressed to late stages, suggesting that changes in ILT3 expression may be associated with ovarian tumor development and progression. The presence of active antitumor immune responses against ovarian tumors at the early stage has been reported earlier [9]. However, despite the presence of an antitumor immune response, OVCAs in most cases, progress to late stages. Although the precise mechanisms of such immune escaping are not known, our results suggest that the enhanced expression of immune inhibitory receptor ILT3 by the ovarian tumors may contribute to the progression of OVCA.

The results of the present study suggest that the expression pattern of ILT3 varies with the different histologic subtypes of ovarian tumors. Significantly high ILT3 staining intensity was observed in serous compared with endometrioid ovarian tumors at early as well as late stages of OVCA. The specific reasons for higher ILT3 expression by serous OVCA are not known. It is possible that higher ILT3 expression will contribute to the faster progression of OVCA by imparting higher immune tolerance to tumors. Serous malignant ovarian tumors are considered aggressive tumors, and increased ILT3 expression may contribute to their faster progression. Similar observations in cancers of other organs were also reported previously [31,34]. Thus, it is possible that ILT3 will contribute to ovarian tumor progression by suppressing antitumor immunity.

In the present study, a portion of the epithelial cells of the normal ovarian surface epithelium above the cortical developing follicles (not all epithelial cells) were positive for ILT3 expression albeit with lower intensity than the epithelium of ovarian tumors. Although the precise reason(s) for such expression is not known, it is possible that ILT3 expressed by surface epithelial cells near cortical follicles will protect them from immune cells by suppression of local antifollicular autoimmune response. Various structures in the developing follicles including the perivitelline membrane, granulosa and theca layers, as well as the degenerated cellular components of postovulatory follicles may appear as "foreign" to the circulating immune cells because these structures were not present during the evolution and maturation of the immune system.

Our understanding regarding the biology and the role of ILT3 in the context of OVCA is very limited, in part, because of the lack of an animal model that develops spontaneous OVCA. Because of the difficulty of detecting OVCA at an early stage, access to patient specimens to study and develop an effective antitumor immunotherapy is difficult and time consuming. Similarities between the spontaneous OVCA in humans and hens in histologic subtypes, risk factors (e.g., incessant ovulation), and expression of several molecular makers of OVCA represent a high probability that results obtained from this study may be translated to clinics. Furthermore, one of the most important advantages of this animal model relative to the possibilities of translating current findings to OVCA in humans is the ability to monitor hens by contrast enhanced ultrasound imaging using equipment and mechanical setting similar to those used in clinics [25,26]. Thus, there will be less variation in imaging parameters between hens and humans because of the use of similar equipment. With the advancement in *in vivo* imaging technology, ligands that bind to the epithelial cells of the ovarian tumor are being developed to use as antitumor therapies, and their effectiveness in tumor ablation can be monitored in this animal model using contrast-enhanced ultrasound scanning [35]. Because the epithelial cells of the tumor in OVCA hens express ILT3, laying hens may be used to test the efficacy of anti-ILT3 drug by molecular-targeted ultrasound imaging of ovarian tissues. Thus, it will bring a significant change in the development of tumor specific therapeutics specially immunoenhancing drugs and lead to the development of treatment modalities for OVCA patients. Taken together, information on ILT3 expression and its association with OVCA progression will aid in the development of anti-ILT3 immunotherapies, which will lay the foundation for clinical studies and may ultimately lead to the development of effective therapies for the treatment of OVCA.

Acknowledgments

The authors thank Chet and Pam Utterback and Doug Hilgendorf, staff of the University of Illinois at Urbana-Champaign Poultry Research Farm, for maintenance of the hens. The authors also thank Sergio Abreu Machado and Syed Tahir Abbas Shah, graduate students, Department of Animal Sciences, University of Illinois at Urbana-Champaign, for helping in hen tissue collection.

References

[1] Jemal A, Siegel R, Xu J, and Ward E (2010). Cancer statistics, 2010. *CA Cancer J Clin* **60**, 277–300.

[2] Goodman MT, Correa CN, Tung KH, Roffers SD, Cheng Wu X, Young JL Jr, Wilkens LR, Carney ME, and Howe HL (2003). Stage at diagnosis of ovarian cancer in the United States, 1992–1997. *Cancer* **97**, 2648–2659.

[3] Ries LA (1993). Ovarian cancer. Survival and treatment differences by age. *Cancer* **71**, 524–529.

[4] Zou W (2006). Regulatory T cells, tumour immunity and immunotherapy. *Nat Rev Immunol* **6**, 295–307.

[5] Beyer M and Schultze JL (2006). Regulatory T cells in cancer. *Blood* **108**, 804–811.

[6] Figdor CG, de Vries IJ, Lesterhuis WJ, and Melief CJ (2004). Dendritic cell immunotherapy: mapping the way. *Nat Med* **10**, 475–480.

[7] Dougan M and Dranoff G (2009). Immune therapy for cancer. *Annu Rev Immunol* **27**, 83–117.

[8] Shu S, Cochran AJ, Huang RR, Morton DL, and Maecker HT (2006). Immune responses in the draining lymph nodes against cancer: implications for immunotherapy. *Cancer Metastasis Rev* **25**, 233–242.

[9] Yigit R, Massuger LF, Figdor CG, and Torensma R (2010). Ovarian cancer creates a suppressive microenvironment to escape immune elimination. *Gynecol Oncol* **117**, 366–372.

[10] Curiel TJ, Coukos G, Zou L, Alvarez X, Cheng P, Mottram P, Evdemon-Hogan M, Conejo-Garcia JR, Zhang L, Burow M, et al. (2004). Specific recruitment of regulatory T cells in ovarian carcinoma fosters immune privilege and predicts reduced survival. *Nat Med* **10**, 942–949.

[11] Li MO, Wan YY, Sanjabi S, Robertson AK, and Flavell RA (2006). Transforming growth factor-β regulation of immune responses. *Annu Rev Immunol* **24**, 99–146.

[12] Kriegel MA, Li MO, Sanjabi S, Wan YY, and Flavell RA (2006). Transforming growth factor-β: recent advances on its role in immune tolerance. *Curr Rheumatol Rep* **8**, 138–144.

[13] Liu Z, Guo B, and Lopez RD (2009). Expression of intercellular adhesion molecule (ICAM)-1 or ICAM-2 is critical in determining sensitivity of pancreatic cancer cells to cytolysis by human γδ-T cells: implications in the design of γδ-T-cell–based immunotherapies for pancreatic cancer. *J Gastroenterol Hepatol* **24**, 900–911.

[14] Roncarolo MG, Bacchetta R, Bordignon C, Narula S, and Levings MK (2001). Type 1 T regulatory cells. *Immunol Rev* **182**, 68–79.

[15] Liu Z, Tugulea S, Cortesini R, and Suciu Foca N (1998). Specific suppression of T helper alloreactivity by allo MHC class I–restricted $CD8^+CD28^-$ T cells. *Int Immunol* **10**, 775–783.

[16] Wei S, Kryczek I, Zou L, Daniel B, Cheng P, Mottram P, Curiel T, Lange A, and Zou W (2005). Plasmacytoid dendritic cells induce $CD8^+$ regulatory T cells in human ovarian carcinoma. *Cancer Res* **65**, 5020–5026.

[17] Kryczek I, Zou L, Rodriguez P, Zhu G, Wei S, Mottram P, Brumlik M, Cheng P, Curiel T, Myers L, et al. (2006). B7-H4 expression identifies a novel suppressive macrophage population in human ovarian carcinoma. *J Exp Med* **203**, 871–881.

[18] Salazar-Onfray F (1999). Interleukin-10: a cytokine used by tumors to escape immunosurveillance. *Med Oncol* **16**, 86–94.

[19] Suciu-Foca N, Feirt N, Zhang QY, Vlad G, Liu Z, Lin H, Chang CC, Ho EK, Colovai AI, Kaufman H, et al. (2007). Soluble Ig-like transcript 3 inhibits tumor allograft rejection in humanized SCID mice and T cell responses in cancer patients. *J Immunol* **178**, 7432–7441.

[20] Kim-Schulze S, Scotto L, Vlad G, Piazza F, Lin H, Liu Z, Cortesini R, and Suciu-Foca N (2006). Recombinant Ig-like transcript 3-Fc modulates T cell responses via induction of Th anergy and differentiation of $CD8^+$ T suppressor cells. *J Immunol* **176**, 2790–2798.

[21] Rodriguez-Burford C, Barnes MN, Berry W, Partridge EE, and Grizzle WE (2001). Immunohistochemical expression of molecular markers in an avian model: a potential model for preclinical evaluation of agents for ovarian cancer chemoprevention. *Gynecol Oncol* **81**, 373–379.

[22] Barua A, Bitterman P, Abramowicz JS, Dirks AL, Bahr JM, Hales DB, Bradaric MJ, Edassery SL, Rotmensch J, and Luborsky JL (2009). Histopathology of ovarian tumors in laying hens: a preclinical model of human ovarian cancer. *Int J Gynecol Cancer* **19**, 531–539.

[23] Viertlboeck BC, Habermann FA, Schmitt R, Groenen MA, Du Pasquier L, and Gobel TW (2005). The chicken leukocyte receptor complex: a highly diverse multigene family encoding at least six structurally distinct receptor types. *J Immunol* **175**, 385–393.

[24] Dennis G Jr, Kubagawa H, and Cooper MD (2000). Paired Ig-like receptor homologs in birds and mammals share a common ancestor with mammalian Fc receptors. *Proc Natl Acad Sci USA* **97**, 13245–13250.

[25] Barua A, Abramowicz JS, Bahr JM, Bitterman P, Dirks A, Holub KA, Sheiner E, Bradaric MJ, Edassery SL, and Luborsky JL (2007). Detection of ovarian tumors in chicken by sonography: a step toward early diagnosis in humans? *J Ultrasound Med* **26**, 909–919.

[26] Barua A, Bitterman P, Bahr JM, Bradaric MJ, Hales DB, Luborsky JL, and Abramowicz JS (2010). Detection of tumor-associated neoangiogenesis by Doppler ultrasonography during early-stage ovarian cancer in laying hens: a preclinical model of human spontaneous ovarian cancer. *J Ultrasound Med* **29**, 173–182.

[27] Giles JR, Olson LM, and Johnson PA (2006). Characterization of ovarian surface epithelial cells from the hen: a unique model for ovarian cancer. *Exp Biol Med (Maywood)* **231**, 1718–1725.

[28] Barua A, Edassery SL, Bitterman P, Abramowicz JS, Dirks AL, Bahr JM, Hales DB, Bradaric MJ, and Luborsky JL (2009). Prevalence of antitumor antibodies in laying hen model of human ovarian cancer. *Int J Gynecol Cancer* **19**, 500–507.

[29] Hong YH, Lillehoj HS, Lee SH, Dalloul RA, and Lillehoj EP (2006). Analysis of chicken cytokine and chemokine gene expression following *Eimeria acervulina* and *Eimeria tenella* infections. *Vet Immunol Immunopathol* **114**, 209–223.

[30] Poschke I, Mougiakakos D, and Kiessling R (2011). Camouflage and sabotage: tumor escape from the immune system. *Cancer Immunol Immunother* **60**, 1161–1171.

[31] Vlad G, Chang CC, Colovai AI, Vasilescu ER, Cortesini R, and Suciu-Foca N (2010). Membrane and soluble ILT3 are critical to the generation of T suppressor cells and induction of immunological tolerance. *Int Rev Immunol* **29**, 119–132.

[32] Cella M, Dohring C, Samaridis J, Dessing M, Brockhaus M, Lanzavecchia A, and Colonna M (1997). A novel inhibitory receptor (ILT3) expressed on monocytes, macrophages, and dendritic cells involved in antigen processing. *J Exp Med* **185**, 1743–1751.

[33] Manavalan JS, Kim-Schulze S, Scotto L, Naiyer AJ, Vlad G, Colombo PC, Marboe C, Mancini D, Cortesini R, and Suciu-Foca N (2004). Alloantigen specific $CD8^+CD28^-$ $FOXP3^+$ T suppressor cells induce $ILT3^+$ $ILT4^+$ tolerogenic endothelial cells, inhibiting alloreactivity. *Int Immunol* **16**, 1055–1068.

[34] Colovai AI, Tsao L, Wang S, Lin H, Wang C, Seki T, Fisher JG, Menes M, Bhagat G, Alobeid B, et al. (2007). Expression of inhibitory receptor ILT3 on neoplastic B cells is associated with lymphoid tissue involvement in chronic lymphocytic leukemia. *Cytometry B Clin Cytom* **72**, 354–362.

[35] Barua A, Bitterman P, Bahr JM, Basu S, Sheiner E, Bradaric MJ, Hales DB, Luborsky JL, and Abramowicz JS (2011). Contrast-enhanced sonography depicts spontaneous ovarian cancer at early stages in a preclinical animal model. *J Ultrasound Med* **30**, 333–345.

Association of Interleukin 16 With the Development of Ovarian Tumor and Tumor-Associated Neoangiogenesis in Laying Hen Model of Spontaneous Ovarian Cancer

Aparna Yellapa, MS, Janice M. Bahr, PhD,† Pincas Bitterman, MD,‡ Jacques S. Abramowicz, MD,§ Seby L. Edassery, MS,* Krishna Penumatsa, PhD,* Sanjib Basu, PhD,|| Jacob Rotmensch, MD,§ and Animesh Barua, PhD*‡§*

Objective: Tumor-associated neoangiogenesis (TAN) is an early event in ovarian tumor development. Interleukin 16 (IL-16) is a proangiogenic cytokine that stimulates production of neoangiogenic factors. The goal of this study was to determine the association of IL-16 with tumor development and ovarian TAN in laying hens, an animal model of spontaneous ovarian cancer (OVCA).

Methods: Sera and ovarian tissues from 3-year-old laying hens were collected and processed for histopathologic, immunoassay, immunohistochemistry, immunoblotting, and molecular biological studies to determine the tissue expression and serum levels of IL-16. Samples were divided into 3 groups based on the diagnosis of the histopathologic ovarian tissue examination, namely, normal (healthy control, n = 81), early (n = 23 including 11 with microscopic OVCA), and late stages (n = 16) of OVCA.

Results: Serum levels of IL-16 were significantly higher in hens with microscopic, early, and late stages of OVCA than normal hens ($P < 0.0001$). The frequencies of IL-16$^+$cells in tumor-bearing ovaries were significantly higher than normal hens ($P < 0.05$). The expression of IL-16 protein and mRNA were stronger in tumor-bearing ovaries than normal ovaries. In addition to ovarian stroma, IL-16 was also expressed by the epithelial cells of the tumor in OVCA hens. Differences in serum levels and ovarian IL-16 expression were not significant among different histological subtypes of OVCA including serous, endometrioid, and mucinous. Similar to the serum levels and ovarian expression of IL-16, the densities of neoangiogenic microvessels were significantly higher in hens with tumor-bearing ovaries than normal hens.

Conclusions: The results of the study suggest that changes in serum levels of IL-16 are associated with tumor development and TAN. Thus, serum IL-16 levels may be an indicator of ovarian TAN at the early stage of OVCA.

Key Words: Interleukin 16, Ovarian tumor, Tumor-associated neoangiogenesis, Ovarian cancer

Received July 5, 2011, and in revised form August 24, 2011.
Accepted for publication September 8, 2011.

(*Int J Gynecol Cancer* 2012;22: 199–207)

*Department of Pharmacology, Rush University Medical Center, Chicago; †Department of Animal Sciences, University of Illinois at Urbana-Champaign; and Departments of ‡Pathology, §Obstetrics and Gynecology, and ||Preventive Medicine (Biostatistics), Rush University Medical Center, Chicago, IL.

Address correspondence and reprint requests to Animesh Barua, PhD, Department of Pharmacology, Laboratory for Translational Research on Ovarian Cancer, Rush University Medical Center, Room # 410, Cohn Bldg, 1735 W Harrison St, Chicago IL 60612. E-mail: Animesh_Barua@rush.edu.

ISSN: 1048-891X
DOI: 10.1097/IGC.0b013e318236a27b

This study was supported by the Idea Development Award from the US Department of Defense (OC#093303) and the Elmer Sylvia and Sramek Foundation (USA).

The authors declare that there are no conflicts of interest.

Nonspecificity of symptoms at an early stage and the lack of an effective early detection test make ovarian cancer (OVCA) a fatal malignancy in women.[1] Circulating levels of CA-125 alone or in combination with transvaginal ultrasound scan did not substantially improve the diagnosis of early-stage OVCA. Thus, an effective early detection test for OVCA remains to be established. Similar to cancers of other organs, tumor-associated neoangiogenesis (TAN) is also an early event during ovarian tumor development, and it plays critical roles in tumor growth and progression.[2,3] Thus, ovarian TAN vessels have the potential to be a target marker for early detection of OVCA. Doppler ultrasound scanning (DUS), a favored method for the detection of ovarian vascularity, cannot detect early ovarian TAN-related microvessels. Although vascular endothelial growth factor is a marker of TAN, it is not specific to OVCA.[4] Thus, for effective early detection of OVCA, either the current detection limit of DUS needs to be improved, or an effective serum marker of TAN needs to be explored.

Cytokines are reported to play putative roles in OVCA progression by enhancing tumor growth or metastasis or modulating the immune system.[5] Interleukin 16 (IL-16) is a cytokine involved in multiple immunopathobiological processes including chemotaxis of immune cells,[6] initiation of inflammatory responses,[7] and production of proangiogenic cytokines.[8] Interleukin 16 is produced mainly by members of the immune system.[6] Recently, IL-16 levels have been reported to be altered in association with several advanced-stage solid tumors (breast, gastrointestinal, uterine renal/bladder, and lung cancers),[9] hematologic malignancies,[10] and nonmalignant diseases including lupus and rheumatoid arthritis. An association between the serum levels of IL-16 and the early ovarian TAN has not yet been reported. If such an association exists, IL-16 may be used as a soluble marker to aid in vivo DUS detection of early ovarian TAN. Because it is difficult to identify patients at the early-stage OVCA, access to the patient's specimen remains a significant barrier to study existence of such an association.

Laying hens are the only widely available and easily accessible animals that develop OVCA spontaneously with a high incidence rate.[11] The histopathology and expression of several markers of OVCA in hens are similar to humans.[11,12] As in humans, IL-16 in chicken is synthesized as a precursor protein (pro–IL-16), with 49% to 52% identity to mammalian homologs.[13] Our goal was to determine whether the serum levels of IL-16 is associated with early-stage ovarian TAN in hens. We tested the hypothesis that serum levels of IL-16 are increased during ovarian tumor development and associated with early ovarian TAN.

MATERIALS AND METHODS

Animals

Commercial strains of 3-year-old white leghorn laying hens (*Gallus domesticus*) were maintained under standard poultry husbandry practices. The incidence of OVCA in hens of this age group is approximately 15% to 20% and is associated with low or complete cessation of egg laying.[14] Hens (n = 120) were selected on the basis of their egg-laying rates (normal or low) and transvaginal ultrasound as reported previously.[14] All experimental procedures were performed according to the Institutional Animal Care and Use Committee–approved protocol.

Tissue Collection and Processing

Serum Samples

Blood was obtained from brachial veins of all hens before they were killed, and the blood was centrifuged (1000*g*, 20 minutes), and serum samples were stored at −80°C.

Gross Ovarian Morphology and Histopathology

Ovarian pathology and tumor staging were performed by gross and histological examination as reported previously.[11] Each normal or tumor-bearing ovary was divided into 4 portions for protein extraction, total RNA collection, and paraffin and frozen embedding for routine histology and immunohistochemical studies as reported previously.[3] Normal ovarian surface epithelial cells or epithelial cells of the tumor in OVCA hens were collected similarly as reported earlier.[15] Samples were classified into 3 groups including normal-, early-, and late-stage OVCA based on the diagnosis of the histopathologic ovarian tissue examination as reported previously.[11]

Preparation of Ovarian Specimen for Biochemical Analysis

Snap-frozen ovarian tissues as well as normal ovarian surface epithelial cells and epithelial cells of the tumor in OVCA hens were homogenized with a Polytron homogenizer (Brinkman Instruments, Westbury, NY) as reported previously[16] and centrifuged, and supernatant was collected; protein content of the extract was measured and stored at −80°C.

Immunoassay

Serum levels of IL-16 were determined by Chicken IL-16 Vetset ELISA Kit (Kingfisher Biotech, St Paul, MN) as per the manufacturer's instructions. Briefly, chicken IL-16 standards or serum samples were added to the wells precoated with anti–chicken IL-16 antibodies followed by the incubation with detection antibody and streptavidin–horseradish peroxidase. Immunoreactions were developed by TMB substrate and stopped by 0.18 M sulfuric acid. The absorbance for each well was recorded by reading the plates at 450 nm in a plate reader (Thermomax; Molecular Devices, Sunnyvale, CA). A standard curve was generated by plotting the optical density values of the standards against their concentrations. Serum IL-16 levels were determined with reference to the standard curve as per manufacturer's instruction using a software program (Softmax Pro, version 1.2.0, software; Molecular Devices). All standards and serum samples were run in duplicate.

Immunohistochemistry

Immunohistochemical localizations of IL-16^{+} cells using anti–IL-16 (Kingfisher Biotech) and ovarian TAN vessels

using anti–smooth muscle actin (SMA) (Invitrogen, Carlsbad, CA) and anti–$\alpha_v\beta3$ integrins (CD51/CD61, clone 23C6; BioLegend, San Diego, CA) antibodies in normal or tumor-bearing ovaries (n = 15 hens each for normal, early [including microscopic] and late stages) were performed as reported previously.[3] The number of hens for each group for immunohistochemical studies was determined based on the power analysis to achieve significant differences in the frequencies of immunopositive cells or microvessels among the 3 pathological groups. These hens were selected from each group randomly based on their reactivity in immunoassay. Double label immunostaining was performed to determine whether IL-16 is expressed by normal ovarian surface epithelium or epithelium of the tumor in OVCA hens. Briefly, frozen sections from normal or tumor-bearing ovaries were immunostained for cytokeratin (a marker of epithelial cell) using anti–cytokeratin 7 antibodies (this antibody was developed against OTN 11 ovarian carcinoma cell lines; Abcam Inc, Cambridge, MA) in the first step and anti–IL-16 antibodies in the second step. Cytokeratin-positive cells were visualized with DAB, and IL-16$^+$ cells were detected by DAB with nickel chloride as reported earlier.[17] Sections were then counterstained with hematoxylin, dehydrated, and covered. In control staining, first antibody was replaced with normal mouse immunoglobulin G, and no immunopositive cell was found on the control slides.

Counting of Immunopositive Cells or Microvessels

The densities of IL-16$^+$ cells, anti-SMA$^+$, and anti-$\alpha_v\beta_3$ integrin$^+$ microvessels were counted from the normal ovarian or tumor stroma of hens using a light microscope attached to a digital imaging software (MicroSuite version 5; Olympus Corporation, Tokyo, Japan). Three sections per ovary were selected. In each section, 5 regions containing a high population of immunopositive microvessels or 5 random areas for IL-16$^+$ cells were used. Frequencies of IL-16$^+$ cells or microvessels in 20,000-μm^2 area were counted at a $\times$40 objective and $\times$10 ocular magnification as reported previously.[3,18] The mean of these counts was considered as the number of immunopositive microvessels or IL-16$^+$ cells in a 20,000-μm^2 area of a section. The mean of 3 sections was considered as the mean of immunopositive vessels or IL-16$^+$ cells in normal or tumor-bearing ovaries.[3]

One-Dimensional Western Blot

Serum samples for Western blotting were selected randomly to represent normal (n = 5), early including microscopic (n = 12), and late stages (n = 12) of OVCA based on their immunoreactivity for IL-16 in immunoassay (enzyme-linked immunosorbent assay). Serum samples were filtered by acetonitrile and chloroform-methanol precipitation and tested by immunoblotting to confirm immunoreactions observed in immunoassay as reported earlier.[16] Similarly, ovarian expression of IL-16 was confirmed by using whole ovarian homogenates and normal ovarian surface epithelial cells or epithelial cells of the tumor in OVCA hens. Immunoreactions on the membrane were visualized as a chemiluminescence product (Super Dura West substrate; Pierce/Thermo Fisher, Rockford, IL), and the image was captured using a Chemidoc CRS (BioRad, Hercules, CA). Chicken recombinant IL-16 protein was used as standard in immunoblotting.

Reverse Transcription–Polymerase Chain Reaction

Interleukin 16 mRNA expression was assessed by semiquantitative reverse transcription–polymerase chain reaction (PCR) as reported previously.[19] For reverse transcription–PCR analyses, serum and tissue samples from 5 normal, 12 early (including microscopic, 4 from each of the serous, endometrioid, and mucinous), and 12 late stages (4 from each of the serous, endometrioid, and mucinous) of OVCA hens were selected based on their reactivity in immunoassay, immunoblotting, and immunohistochemistry. Hen-specific IL-16 primers were designed by Oligoperfect Designer software (Invitrogen) using the IL-16 sequence from the NCBI (GeneBank NM_204352.3). The forward primer was 5-TCTCTGC TTTCCCCTGAA-GA, and the reverse primer was 5-GTC CATTGGGAAACACCT-TG located between exons 4 and 6. β-Actin was used as the endogenous control with a forward primer of TGCGTGACATCAAGGAGAAG and a reverse primer of ATGCCAGGGTACATTGTGGT. The expected base pair size for the IL-16 amplicon was 199 base pairs and for β-actin was 300 base pairs. Polymerase chain reaction amplicons were visualized in a 3% agarose gel (Pierce/Thermo Fisher) in Tris-acetate-EDTA buffer and stained with ethidium bromide. The image was captured using a ChemiDoc XRS system (BioRad).

Statistical Analysis

The differences in the frequencies of IL-16$^+$ cells and immunopositive microvessels among normal ovaries, tumor-bearing ovaries in hens with early-stage and late-stage OVCA were assessed by analysis of variance, F tests, and the alternative nonparametric Kruskal-Wallis tests. Then pairwise comparisons between the groups (normal-, early-, and late-stage OVCA) by 2-sample *t* tests and alternative Mann-Whitney tests were performed. All reported *P* values are 2-sided, and $P < 0.05$ was considered significant. Statistical analyses were performed with SPSS (PASW) version 18 software (IBM Inc, Armonk, NY).

RESULTS

Ovarian Morphologic and Histological Features

Gross Morphology

Hens with a fully functional ovary contained 5 to 6 developing preovulatory follicles (Fig. 1A). Only 1 or 2 such follicles were present in the ovaries of low-laying healthy hens. In normal hens that stopped egg laying, ovaries and oviducts were regressed without any detectable abnormality. Solid tissue masses either limited to a small part or whole ovary and with or without ascites were observed in 12 hens and classified as hens with early-stage OVCA (Fig. 1B). In 16 hens, tumor metastasized to abdominal organs with moderate

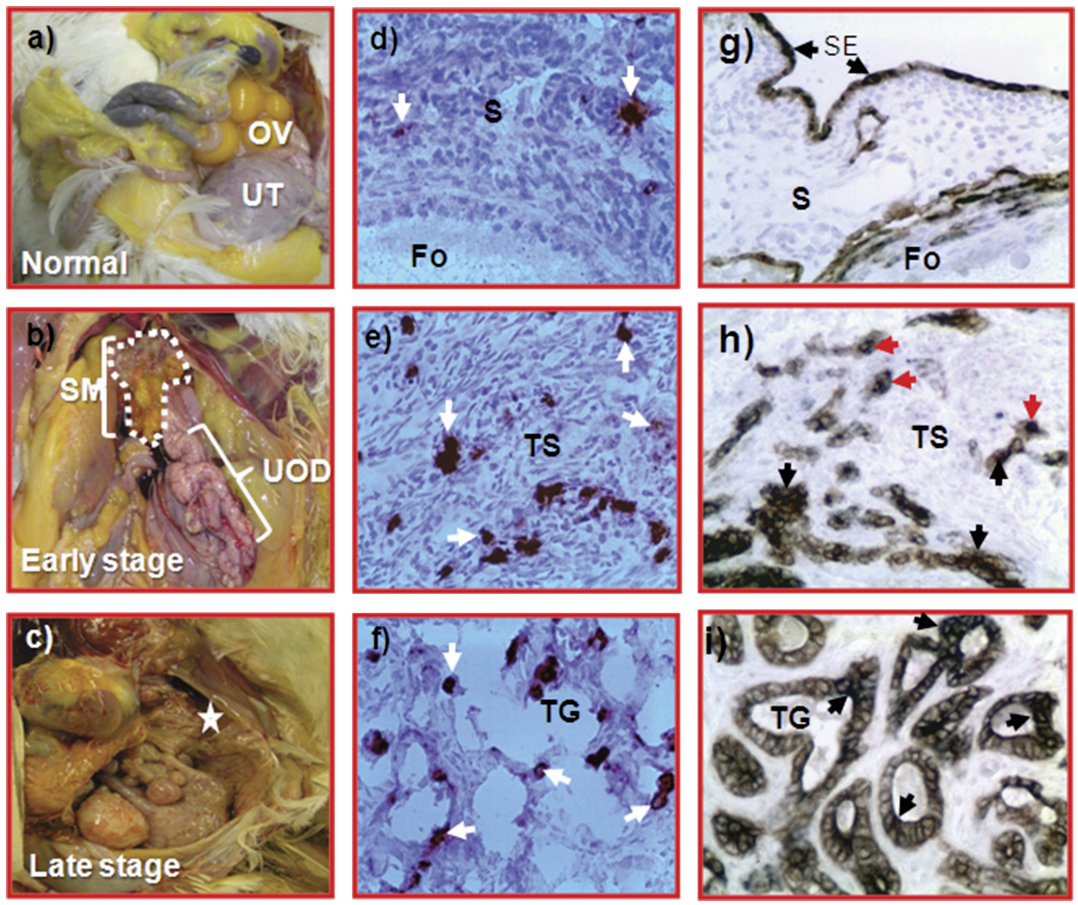

FIGURE 1. Gross morphology and immunolocalization of IL-16$^+$ cells in normal ovaries and ovaries with tumor in laying hens. A–C, Gross morphology of normal ovary or ovaries with tumors in hens. A, A normally laying hen ovary contains a hierarchy of multiple large preovulatory follicles with active oviduct. B, Ovarian cancer at an early stage in a laying hen. Tumor mass is limited to the ovary (shown in a dotted line), and the oviduct is atrophied. C, Late-stage OVCA in a laying hen. Tumor is metastasized to distant organs with accompanied profuse ascites (*). D–F, Interleukin 16–expressing cells in the stroma of a normal ovary or ovaries with tumors in laying hens. Frozen sections from ovaries shown in A to C were immunostained for IL-16–expressing cells. Cells expressing IL-16 are round or irregularly shaped and seen in the normal ovarian stroma as well as in the vicinity of tumors. D, Very few positive cells are seen in the stroma of normal ovary. E and F, Interleukin 16 expression in early (E) and late (F) stages of OVCA in laying hens. A number of epithelial cells (not all) of the tumor in the ovaries were also positive for IL-16 expression (E–F). Compared with normal ovary (D), more IL-16$^+$ cells are seen in the stroma of the ovaries with tumor (E–F) in OVCA hens. G-I, Expression of IL-16 by ovarian epithelium in hens with or without OVCA. Frozen sections were immunostained for cytokeratin 7 (a specific marker for epithelial cell) in the first step to confirm ovarian epithelial cells and for IL-16 in the second step using DAB and DAB and nickel chloride, respectively. Cytokeratin 7–positive epithelial cells expressing IL-16 appeared as gray-black (examples shown in black arrows) compared with light brown non–IL-16–expressing cytokeratin 7–positive cells. G, Interleukin 16 expression by normal ovarian surface epithelium. H and I, Interleukin 16 expression by the epithelial cells of the tumor in hens with early (H) and late stages (I) of OVCA. In addition to the epithelial cells, some rounded cells (with T cell–like phenotype) were stained dark green for IL-16 only (red arrows) in the stroma of the ovaries with tumor (H). S, Stroma; SE, surface epithelium, SM, solid mass, TG, tumor gland; TS, tumor stroma, UOD, upper oviduct, UT, uterus. *Ascites. Original magnification ×40. Arrows indicate the examples of immunopositive cells.

to profuse ascites and classified as hens with late-stage OVCA (Fig. 1C).

Histopathology

Ovarian tumors in 28 hens that had solid mass limited to the ovaries (n = 12, early stage) or metastasized to other organs (n = 16, late stage) were confirmed by routine histology. However, tumor-associated microscopic features were also found during histological examinations in 11 additional hens (hens with microscopic OVCA) that had no grossly detectable solid mass in the ovary and were grouped in early-stage OVCA. Thus, a total of 23 (12 + 11) hens had early and

16 had late stage of OVCA, whereas 81 hens were normal. Tumors were typed as serous (n = 17), endometrioid (n = 12), mucinous (n = 8), and clear cell (n = 1) as well as mixed (n = 1, seromucinous) as reported previously.[11]

Tissue Expression and Serum Levels of IL-16

Immunohistochemical Detection of Ovarian IL-16 Expression

Rounded (T lymphocyte–like) to irregularly shaped (macrophage-like appearances) IL-16$^+$ cells were detected in the stroma of normal or tumor-bearing ovaries and in the tumor vicinity including spaces between tumor glands (Figs. 1D–F). A number of epithelial cells (not all) in normal or tumor glands were also positive for IL-16 (Figs. 1D–F), which was confirmed by double immunostaining for IL-16 together with cytokeratin (Figs. 1G–I). The frequencies of IL-16$^+$ cells in the stroma of tumor-bearing ovaries in hens with early-stage (mean, 15.88 [SD, 3.33] cells/20,000-μm^2 area) and late-stage (19.5 [SD, 4.90] cells/20,000-μm^2 area) OVCA were significantly ($P < 0.05$) higher than in the ovarian stroma of normal hens (5.24 [SD, 1.38] cells/20,000-μm^2 area). Thus, epithelial cells in normal ovaries or tumor-bearing ovaries also express IL-16.

Immunoassay for Serum IL-16 Levels

Mean concentration of serum IL-16 was 259.91 (SD, 71.90) pg/mL in normal hens (n = 50). Compared with normal hens, the mean concentration of serum IL-16 was significantly higher ($P < 0.0001$) in hens with microscopic OVCA (531.85 [SD, 193.77] pg/mL) and increased further in hens with early (739.55 [SD, 148.75] pg/mL) and late stages (767.04 [SD, 264.37] pg/mL) of OVCA (Fig. 2). Although compared with hens with microscopic OVCA, serum IL-16 levels were significantly higher in hens with early ($P < 0.009$) and late stages ($P < 0.004$) of OVCA, differences in serum IL-16 levels were not significant between the early- and late-stage OVCA as well as among the different histological subtypes of OVCA.

Immunoblotting for IL-16 Protein in Serum Samples and Ovarian Tissues

Immunoreactivity of serum IL-16 detected by immunoassay was confirmed with immunoblotting using serum samples from selected hens representative of each group including normal-, early-, and late-stage OVCA. As expected, a band at approximately 15 to 18 kd was detected in recombinant IL-16 samples (data not shown), whereas a band of approximately 60 to 65 kd (equivalent to the homotetramer of recombinant IL-16 peptide) was detected in the serum from normal hens or hens with OVCA (Fig. 3A).

Expression of ovarian IL-16 was also confirmed by immunoblotting using ovarian epithelium or whole ovarian homogenates from normal hens or hens with OVCA. Interleukin 16 protein from whole ovarian homogenates in hens with OVCA showed moderate to intense immunoreactivity

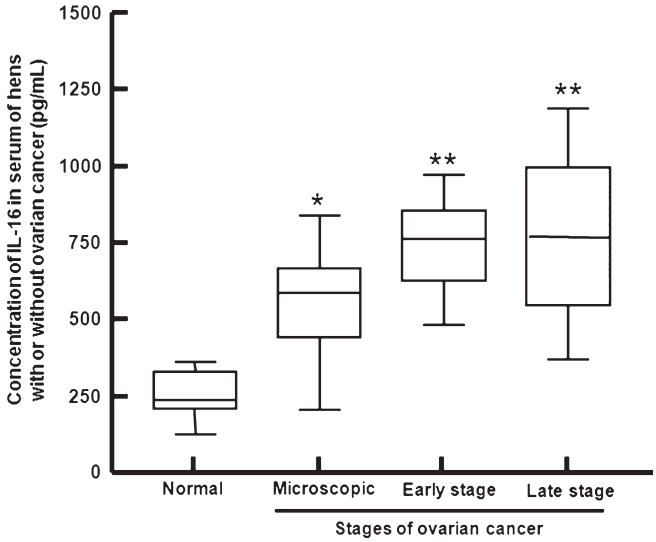

FIGURE 2. Interleukin 16 levels in serum of hens with or without ovarian tumors displayed as box and whiskers (expressed in pg/mL). The median, range (whiskers), and 25th to 75th percentiles (box) are shown. Serum samples from normal hens were used as experimental controls. Compared with control hens (n = 50), serum IL-16 levels increased significantly ($P < 0.0001$) in hens with microscopic (n = 11), early (n = 12), and late (n = 16) stages of OVCA. *Significant differences in the serum IL-16 levels between normal hens and hens with microscopic OVCA; **same between the hens with microscopic OVCA and hens with early or late stages of OVCA.

(Fig. 3B). In contrast, either a very weak or no immunoreactive band was seen for whole ovarian homogenates from healthy hens. Similarly, stronger IL-16 immunoreactivity was observed for the epithelial cells of the tumor in OVCA hens than that of normal ovarian surface epithelial cells (Fig. 3B). These results confirm the immunohistochemical observation that ovarian surface epithelial cells in normal hens and epithelial cells of the tumor in OVCA hens may be a source of IL-16 proteins in hens.

Expression of IL-16 Messenger RNA

Interleukin 16 messenger RNA (mRNA) expression confirmed the observed variations in serum IL-16 levels and ovarian IL-16 expression among normal and OVCA hens. Hens with ovarian tumors showed strong amplification signal for IL-16 (Fig. 3C) and differences were not observed in IL-16 mRNA expression among different histological subtypes of OVCA. In contrast, IL-16 mRNA expression was weak for whole ovarian homogenates from normal hens. Similar patterns were also observed for surface epithelial cells of the normal ovaries or epithelial cells of the tumor in OVCA hens. Overall, compared with normal hens, strong amplification of IL-16 mRNA was observed in OVCA hens as observed for immunoreactivities in immunoassay and immunoblotting.

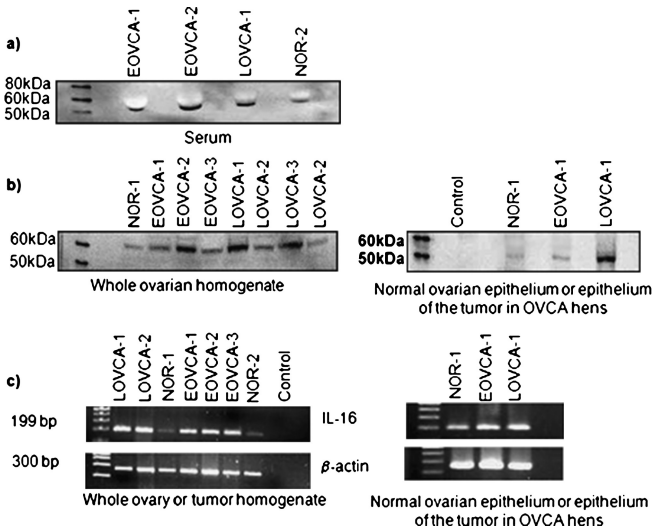

FIGURE 3. Examples of immunoreactive IL-16 protein (A–B) or mRNA expression (C) in the sera and homogenates of whole ovarian or ovarian epithelium from normal hens (NOR) or epithelium of the tumor in hens with early (EOVCA) and late (LOVCA) stages of OVCA by 1-dimensional Western blotting (1D-WB) and semiquantitative PCR, respectively. 1D-WB (A–B): Immunoreactive IL-16 proteins of 55- to 60-kd molecular weight were detected in sera and homogenates of ovaries from normal hens or hens with ovarian tumors as well as epithelium of the tumor in OVCA hens. Compared with sera and ovaries from normal hens, relatively stronger immunoreactive bands for IL-16 proteins were observed in hens with OVCA. No immunoreactive band was detected in the negative control in which protein sample was omitted. Reverse transcription–PCR (C): mRNA expression was detected in the extract from whole ovarian homogenate or epithelium of the tumor in OVCA hens. Compared with the weak expression by normal ovaries, strong expression of IL-16 mRNA was observed in homogenates of ovarian tumors and epithelium of the tumor in hens with early- and late-stage OVCA. No IL-16 mRNA expression was detected in negative control in which mRNA sample was omitted.

Expression of Angiogenic Markers

Immunopositive microvessels (anti-SMA$^+$ and anti-$\alpha_v\beta_3$ integrin$^+$) were detected in both normal ovaries (n = 15) and ovarian tumors (n = 15 hens each for early- and late-stage OVCA). In normal hens, the wall of immunopositive ovarian vessels, in most cases, was thick, complete, and continuous with intense staining. A few microvessels were also seen in the theca layers of the follicles of normal hens, indicating active sites of physiological angiogenesis associated with follicular development (Fig. 4A). In contrast, most of the immunopositive microvessels in tumor-bearing ovaries were leaky, discontinuous, or incomplete with thin vessel walls. In OVCA hens, more immunopositive microvessels were seen in tumor vicinity and in the stroma adjacent to the tumors (Figs. 4B, C). The frequencies of immunopositive microvessels were significantly ($P < 0.0001$) higher (12.77 [SD, 2.19] anti-SMA and 6.77 [SD, 3.00] anti–$\alpha_v\beta_3$ integrins$^+$ microvessels in 20,000-μm^2 area of tissues) in early-stage OVCA hens than normal hens (5.06 [SD, 1.46] anti-SMA and 2.7 [SD, 0.84] anti–$\alpha_v\beta_3$ integrins$^+$ microvessels in 20,000-μm^2 area of tissues) (Fig. 5). Their frequencies increased further ($P < 0.0001$) in hens with late-stage OVCA (19.39 [SD, 1.95] anti-SMA and 9.97 [SD, 1.65] anti–$\alpha_v\beta_3$ integrins + microvessels in 20,000-μm^2 area of tissues).

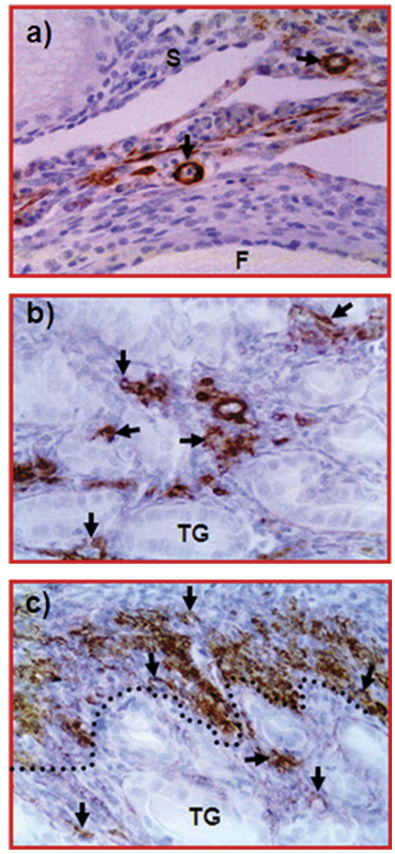

FIGURE 4. Immunolocalization of ovarian microvessels in normal ovary or ovaries with tumor in laying hens. A, Ovarian section from a normal hen. Few immunopositive microvessels are seen in the ovarian stroma. B, Section of a hen's ovary with early-stage OVCA. Compared with the normal ovary, more immature immunopositive microvessels are present in the spaces between tumor glands. C, Section of an ovary with tumor from a hen with late-stage OVCA. Compared with the normal ovary and early-stage OVCA, many microvessels are seen in between tumor glands as well as in the stroma adjacent to the tumor, indicating that tumor angiogenesis precedes tumor progression (separated by an imaginary dotted line). Arrows indicate examples of immunopositive microvessels. F, Follicle; S, stroma; TG, tumor gland.

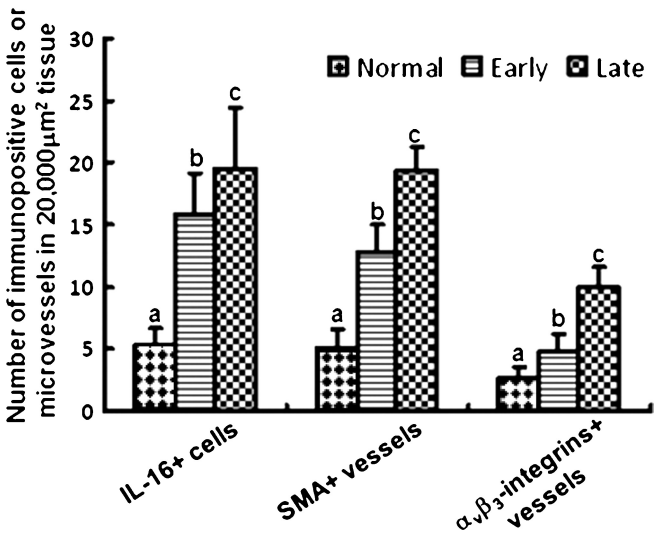

FIGURE 5. Changes in the ovarian IL-16 expression are associated with the increase in the frequencies of ovarian tumor-associated microvessels. The frequencies of immunopositive IL-16 cells or microvessels are expressed as the mean (SD) in 20,000-μm^2 area. As compared with normal hens (n = 15 hens), the frequencies of the IL-16$^+$ cells as well as angiogenic microvessels were significantly increased in hens with OVCA (n = 15 hens each for early including microscopic and late stages of OVCA). The increase in the frequency of ovarian IL-16–expressing cells is associated with the increase in the frequencies of SMA and $\alpha_v\beta_3$ integrin–expressing microvessels. Bars with different letters indicate significant differences ($P < 0.001$) among different pathological categories in IL-16$^+$ cell, SMA$^+$, or $\alpha_v\beta_3$ integrins expressing microvessel groups.

Similar to serum IL-16 levels, the densities of immunopositive microvessels were also increased with the development of OVCA in hens.

DISCUSSION

This is the first report that serum levels and tissue expression of IL-16 increase significantly in association with the development and progression of ovarian TAN in laying hens, a preclinical animal model of spontaneous OVCA. These results suggest that serum IL-16 levels may be a potential indicator of early-stage ovarian TAN and may be useful in combination with conventional markers including vascular endothelial growth factor to detect ovarian TAN.

Precise molecular mechanism of the initiation and regulation of ovarian TAN is not well understood. Involvement of several cytokines and growth factors in the development of TAN has been reported.[5] Interleukin 16 was reported to be involved[9] in lymphoid and ovarian malignancies,[5,10] but none of these reports examined its association with early stages of malignancies. As in humans,[5] the present study showed that IL-16 in hen serum and ovarian tissues also exists in the active homotetramer form. In this study, compared with normal hens, serum levels and tissue expression of IL-16 increased significantly in OVCA hens including microscopic OVCA. The reason(s) for this increase in IL-16 levels in OVCA hens is not known. However, this study suggests that tumor-associated increase in IL-16 level can be detected in serum even before the tumor becomes detectable by TUVS (microscopic OVCA). Furthermore, this increase was correlated with the increased density of TAN-related microvessels. Thus, increased serum IL-16 levels, as observed in hens with early-stage OVCA, may represent an effective serum indicator of early-stage ovarian TAN.

The sources of serum IL-16 are not yet fully known, and published reports are very limited.[20,21] In addition to the immune cells, IL-16 has been reported to be secreted by bronchial epithelium in humans.[20,21] In this study, normal ovarian surface epithelial cells and epithelial cells of the tumor in OVCA hens were positive for IL-16 expression, suggesting that these tissues may also be a source of serum IL-16. Double immunohistochemical labeling showed the expression of IL-16 by the surface epithelial cells of the normal ovaries and epithelial cells of the tumor in OVCA hens, which was further supported by IL-16 protein and mRNA expression. These results are consistent with the previous report that bronchial and tracheal epithelial cells also secrete IL-16.[21] Thus, normal ovarian surface epithelial cells and epithelial cells of the tumor in OVCA hens were also a source of IL-16, and secretion of IL-16 by the epithelial cells of the tumor may be one of the reasons for elevated serum IL-16 levels in OVCA hens including those with microscopic OVCA.

Although the physiological significance of epithelial cell–derived IL-16 in the pathogenesis of OVCA is not clear, it is possible that IL-16 may be involved in the development and progression of OVCA. First, the positive correlation between the increase in IL-16 levels and the frequency of TAN vessels in OVCA hens suggests a proangiogenic role of IL-16 in the progression of ovarian TAN. A proangiogenic role of IL-16 has also been reported in humans.[8] Second, increased expression of IL-16 by epithelial cells of the tumor in OVCA hens and increased levels of serum IL-16 in hens with microscopic OVCA even before the tumor becomes detectable suggest that serum IL-16 levels may also be an indicator of malignant ovarian transformation. Thus, it is possible that IL-16 secreted by the epithelial cells of the tumor in OVCA hens may contribute to ovarian TAN required for tumor growth and may be an effective indicator of ovarian tumorigenesis.

Because of the difficulty of detecting OVCA at an early stage, access to patient specimens to study and develop an early detection test is difficult and time consuming. Because of the similarities between the spontaneous OVCA in humans and hens including histological subtypes, molecular pathways, risk factors (eg, incessant ovulation), and expression of several molecular markers of OVCA, there is a high probability that the results obtained from the OVCA studies in laying hens may be translated to clinics. Moreover, one of the most important advantages relative to the translationalities of the current findings is that OVCA development in

hens can be monitored by contrast-enhanced ultrasound imaging using equipment and mechanical setting similarly used in clinics.[3,14] Thus, there will be least variation on imaging parameters between hens and humans because of the equipment. With the advancement in in vivo imaging technology, ligands that bind to the epithelial cells of the tumor in OVCA hens are being developed to use in conjunction with microbubbles for contrast-enhanced ultrasound scanning to facilitate early OVCA detection.[18] As the epithelial cells of the tumor in OVCA hens express IL-16, it may be used as a target for contrast-enhanced ultrasound imaging and will increase the sensitivity of ultrasound scanning detection of OVCA together with serum levels of IL-16. Thus, it will bring a significant change in imaging paradigms and improve the specificity of ultrasound scanning. It will also be possible to determine the time between the tumor-associated elevation of IL-16 in serum and the earliest detection of tumor by contrast-enhanced ultrasound scanning. This information will enable to detect OVCA at an early stage and lead to the development treatment modalities for OVCA patients. In addition, current findings will also be useful in developing ovarian tumor-associated anti–IL-16 therapies and can be tested in laying hens. Taken together, information on the association of serum and tissue expression of IL-16 with the early detection of OVCA and the potential development of anti–IL-16–based therapies in laying hens will establish the foundation for clinical studies that may ultimately lead to the development of an effective diagnostic test and therapies for OVCA at an early stage.

One of the limitations of the present study is that it did not examine the serum levels and tissue expression of IL-16 in ovarian benign tumors. Thus, exclusion of ovarian benign tumors from the study may limit the translational significance of the findings that serum IL-16 levels may be used as a biomarker for early detection of OVCA. However, serum levels of IL-16 were reported to be significantly higher in patients with prostate cancer than patients with benign prostatic hyperplasia.[22] Therefore, to evaluate the effectiveness of serum IL-16 as a biomarker for early OVCA detection or as a target for imaging of ovarian tumors in patients with early-stage OVCA, present observations need to extend to the investigations on benign ovarian tumors and other benign conditions associated with de novo angiogenesis or IL-16 elevations.

The laying hen is a suitable model to study the role of IL-16 in the pathogenesis of OVCA. With the emergence of newer in vivo imaging technologies, effective targets in the tumor in OVCA hens are being identified to be detected by targeted contrast-enhanced ultrasound imaging to facilitate early OVCA detection. As the epithelial cells of the tumor in OVCA hen express IL-16, these cells may be used as a target for such molecular targeted ultrasound imaging. Thus, serum IL-16 levels together with ultrasound imaging of ovarian tumor-associated IL-16 expression may constitute an effective test for early OVCA. Laying hens are also a suitable model for the development of ultrasound contrast agents for OVCA detection.[18] Finally, the laying hen may also be used to test the efficacy of anti–IL-16 therapies for effective prevention of ovarian TAN.

ACKNOWLEDGMENTS

The authors thank Dr Judith L. Luborsky, PhD, Rush University Medical Center, for her suggestions and comments on the manuscript. They thank Chet and Pam Utterback and Doug Hilgendorf, staff of the University of Illinois at Urbana-Champaign Poultry Research Farm, for maintenance of the hens. They also thank Sergio Abreu Machado and Syed Tahir Abbas Shah, graduate students, Department of Animal Sciences, University of Illinois at Urbana-Champaign, for helping in hen tissue collection.

REFERENCES

1. Jemal A, Siegel R, Xu J, et al. Cancer statistics, 2010. *CA Cancer J Clin*. 2010;60:277–300.
2. Folkman J. What is the evidence that tumors are angiogenesis dependent? *J Natl Cancer Inst*. 1990;82:4–6.
3. Barua A, Bitterman P, Bahr JM, et al. Detection of tumor-associated neoangiogenesis by Doppler ultrasonography during early-stage ovarian cancer in laying hens: a preclinical model of human spontaneous ovarian cancer. *J Ultrasound Med*. 2010;29:173–182.
4. Ramakrishnan S, Subramanian IV, Yokoyama Y, et al. Angiogenesis in normal and neoplastic ovaries. *Angiogenesis*. 2005;8:169–182.
5. Nash MA, Ferrandina G, Gordinier M, et al. The role of cytokines in both the normal and malignant ovary. *Endocr Relat Cancer*. 1999;6:93–107.
6. Center DM, Kornfeld H, Cruikshank WW. Interleukin-16. *Int J Biochem Cell Biol*. 1997;29:1231–1234.
7. Cruikshank WW, Kornfeld H, Center DM. Interleukin-16. *J Leukoc Biol*. 2000;67:757–766.
8. Mathy NL, Scheuer W, Lanzendorfer M, et al. Interleukin-16 stimulates the expression and production of pro-inflammatory cytokines by human monocytes. *Immunology*. 2000;100:63–69.
9. Kovacs E. The serum levels of IL-12 and IL-16 in cancer patients. Relation to the tumour stage and previous therapy. *Biomed Pharmacother*. 2001;55:111–116.
10. Bellomo G, Allegra A, Alonci A, et al. Serum levels of interleukin-16 in lymphoid malignancies. *Leuk Lymphoma*. 2007;48:1225–1227.
11. Barua A, Bitterman P, Abramowicz JS, et al. Histopathology of ovarian tumors in laying hens: a preclinical model of human ovarian cancer. *Int J Gynecol Cancer*. 2009;19:531–539.
12. Rodriguez-Burford C, Barnes MN, Berry W, et al. Immunohistochemical expression of molecular markers in an avian model: a potential model for preclinical evaluation of agents for ovarian cancer chemoprevention. *Gynecol Oncol*. 2001;81:373–379.
13. Min W, Lillehoj HS. Identification and characterization of chicken interleukin-16 cDNA. *Dev Comp Immunol*. 2004;28:153–162.
14. Barua A, Abramowicz JS, Bahr JM, et al. Detection of ovarian tumors in chicken by sonography: a step toward early diagnosis in humans? *J Ultrasound Med*. 2007;26:909–919.
15. Giles JR, Olson LM, Johnson PA. Characterization of ovarian surface epithelial cells from the hen: a unique model for ovarian cancer. *Exp Biol Med (Maywood)*. 2006;231:1718–1725.
16. Barua A, Edassery SL, Bitterman P, et al. Prevalence of antitumor antibodies in laying hen model of human ovarian cancer. *Int J Gynecol Cancer*. 2009;19:500–507.

17. Penumatsa K, Edassery SL, Barua A, et al. Differential expression of aldehyde dehydrogenase 1a1 (ALDH1) in normal ovary and serous ovarian tumors. *J Ovarian Res*. 2010;3:28.
18. Barua A, Bitterman P, Bahr JM, et al. Contrast-enhanced sonography depicts spontaneous ovarian cancer at early stages in a preclinical animal model. *J Ultrasound Med*. 2011;30:333–345.
19. Hong YH, Lillehoj HS, Lee SH, et al. Analysis of chicken cytokine and chemokine gene expression following *Eimeria acervulina* and *Eimeria tenella* infections. *Vet Immunol Immunopathol*. 2006;114:209–223.
20. Wu D, Cruikshank WW, Kornfeld H, et al. Detection of IL-16 in normal bronchial epithelial cell line after cytokine modulation. *Am J Respir Cell Mol Biol*. 1996;153:A208.
21. Arima M, Plitt JR, Stellano C, et al. The expression of lymphocyte chemoattractant factor (LCF) in human bronchial epithelial cells. *J Allergy Clin Immunol*. 1996;97:443.
22. Zhang L, Sun SK, Shi LX, et al. Serum cytokine profiling of prostate cancer and benign prostatic hyperplasia using recombinant antibody microarray [in Chinese]. *Zhonghua Nan Ke Xue*. 16:584–588.

American Society of Clinical Oncology
www.asco.org

Use of contrast-enhanced ultrasound imaging with microbubbles targeted to $\alpha_v\beta_3$ integrins to enhance detection of early-stage ovarian tumors.

Sub-category:
Ovarian Cancer

Category:
Gynecologic Cancer

Meeting:
2011 ASCO Annual Meeting

Session Type and Session Title:
General Poster Session, Gynecologic Cancer

Abstract No:
5076

Citation:
J Clin Oncol 29: 2011 (suppl; abstr 5076)

Author(s):
A. Barua, A. Yellapa, P. Bitterman, J. M. Bahr, S. Sharma, D. B. Hales, J. L. Luborsky, J. S. Abramowicz; Rush University Medical Center, Chicago, IL; University of Illinois at Urbana-Champaign, Urbana, IL; Southern University of Illinois at Carbondale, Carbondale, IL

Abstracts that were granted an exception in accordance with ASCO's Conflict of Interest Policy are designated with a caret symbol (^) here and in the printed Proceedings.

Abstract Disclosures

Abstract:

Background: Lack of an early detection test makes ovarian cancer (OVCA) a lethal gynecological malignancy. Tumor associated neo-angiogenesis (TAN) is an early event in tumor development and represents a potential target for early detection. Traditional transvaginal ultrasound (TVUS) cannot detect TAN at early stage. The goal of this pilot study was to examine the enhancement of TVUS using $\alpha_v\beta_3$ integrins targeted microbubble ultrasound contrast agent (UCA) in laying hens, a preclinical spontaneous model of human OVCA. **Methods:** 3-4 years old hens (n=50) were selected randomly and scanned continuously by TVUS before, during and after UCA (Visister-integrins, Targeson Inc. CA) injection at brachial veins. UCA was visualized using a low mechanical index contrast imaging pulse sequence. All pre- and post-contrast injection images were archived and analyzed off-line. Gross diagnosis was recorded at euthanasia and tissues were processed for histology. Tumors and their types were confirmed by routine histology. TAN markers (SMA and $\alpha_v\beta_3$ integrins) were detected by immunohistochemistry. TAN vessels were counted and correlation with ultrasound prediction was examined. **Results:** $\alpha_v\beta_3$-integrins targeted UCA enhanced the visualization of ovarian tumors significantly in laying hens. At gray scale, UCA bounded areas appeared as a ring on the ovarian surfaces of 8 of 50 hens and were suspected for ovarian tumors. Tumors were confirmed in all hens predicted to have OVCA. In 7 hens tumors were early stage and in one hen the tumor metastasized to the oviduct. A microscopic lesion was found in one hen which was not detected by ultrasound imaging. Thus 9 of 50 hens had ovarian tumors and UCA detected approximately 88% at early stages. The frequency of immunopositive TAN vessels (SMA and $\alpha_v\beta_3$ integrins positive) were significantly higher in OVCA hens than normal hens ($P<0.05$) and was positively correlated (0.86, $P< 0.05$) with ultrasound prediction. **Conclusions:** Our results demonstrate that UCA targeting $\alpha_v\beta_3$ integrin enhanced TVUS detection of early stage ovarian tumors in a pre-clinical model and may form the foundation for a clinical study. Support: Department of Defense (#09-3303), Sramek Foundation.

▸ **Associated Presentation(s):**

1. Use of contrast-enhanced ultrasound imaging with microbubbles targeted to αvβ3 integrins to enhance detection of early-stage ovarian tumors.

Meeting: 2011 ASCO Annual Meeting

Presenter: Animesh Barua
Session: Gynecologic Cancer (General Poster Session)

Other Abstracts in this Sub-Category:

1. A phase II study to evaluate the efficacy and safety of catumaxomab as consolidation treatment in patients with epithelial ovarian cancer in second or third complete remission.

Meeting: 2011 ASCO Annual Meeting Abstract No: TPS195 First Author: A. M. Oaknin
Category: Gynecologic Cancer - Ovarian Cancer

2. Establishing a molecular taxonomy for epithelial ovarian cancer (EOC) from 363 formalin-fixed paraffin embedded (FFPE) specimens.

Meeting: 2011 ASCO Annual Meeting Abstract No: 5000 First Author: C. Gourley
Category: Gynecologic Cancer - Ovarian Cancer

3. Effect of screening on ovarian cancer mortality in the Prostate, Lung, Colorectal, and Ovarian (PLCO) cancer randomized screening trial.

Meeting: 2011 ASCO Annual Meeting Abstract No: 5001 First Author: S. S. Buys
Category: Gynecologic Cancer - Ovarian Cancer

More...

Abstracts by A. Barua:

1. Use of contrast-enhanced ultrasound imaging with microbubbles targeted to $\alpha_v\beta_3$ integrins to enhance detection of early-stage ovarian tumors.

Meeting: 2011 ASCO Annual Meeting Abstract No: 5076 First Author: A. Barua
Category: Gynecologic Cancer - Ovarian Cancer

More...

Presentations by A. Barua:

1. Use of contrast-enhanced ultrasound imaging with microbubbles targeted to αvβ3 integrins to enhance detection of early-stage ovarian tumors.

Meeting: 2011 ASCO Annual Meeting
Presenter: Animesh Barua, PhD
Session: Gynecologic Cancer (General Poster Session)

More...

***Educational Book Manuscripts by A. Barua*:**

No items found.

Print this Page

Presentation Abstract

Abstract Number:	3190
Presentation Title:	Interleukin (IL-16) and tumor associated neo-angiogenesis detects ovarian cancer at early stage
Presentation Time:	Tuesday, Apr 05, 2011, 8:00 AM -12:00 PM
Location:	Exhibit Hall A4-C, Poster Section 13
Poster Section:	13
Poster Board Number:	27
Author Block:	Aparna Yellapa[1], Jacques S. Abramowicz[1], Pincas Bitterman[1], Janice M. Bahr[2], Michael J. Bradaric[1], Seby L. Edassery[1], Sameer Sharma[1], Animesh Barua[1]. [1]Rush University Medical Center, Chicago, IL; [2]University of Illinois at Urbana-Champaign, Champaign, IL

Abstract Body:

Background: The lack of an early detection test is one of the reasons of high mortality rate of women due to epithelial ovarian cancer (OVCA). Understanding the pathogenesis and progression of OVCA is essential to establish an effective early detection test. Tumor associated -immuno-chemotaxis (TAI) and -neoangiogenesis (TAN) are the two earlier events in tumor development. CD8+ T cells in tumor vicinity produce immune-chemotactic IL-16 cytokines which stimulates the production of pro-angiogenic cytokines responsible for TAN. Ovarian TAI and TAN represent potential target for an effective early detection test. Access to patients at early stage OVCA is very difficult and laying hens develop spontaneous OVCA with histopathology similar to humans.
Objectives: The goal of the present study was to determine the feasibility of markers of ovarian TAI and TAN in detecting early stage OVCA in laying hens.
Materials and Methods: 3 years old laying hens (normal, low or stopped egg-laying) were scanned by Ultrasound, sera were collected, hens were euthanized and ovarian tissues were processed for paraffin and frozen sections, and mRNA extraction. Ovarian tumor stages were confirmed at gross and routine histology. Samples were divided into 4 groups namely normal (control), early stage OVCA [microscopic or tumors limited to the ovaries], late stage OVCA, with non-tumor ovarian abnormalities (atrophied ovaries). Sera were tested for IL-16 levels by ELISA and confirmed by 2D-Western blot (WB). Ovarian expression of TAN markerS (VEGF) and, neoangiogenic microvessel density (MVD) as well as IL-16 mRNA was determined.
Results: The population of CD8+ T cells and the serum IL-16 levels were significantly higher in tumor hens ($P < 0.05$) than normal hens. Significant increase in IL-16 levels in hens with microscopic tumor (undetectable at gross examination) suggesting that serum IL-16 may be a potential indicator of ovarian tumors at very early stage. Differences in serum IL-16 levels were not observed between hens with non-tumor ovarian pathology and normal hens suggesting that increased serum IL-16 levels in OVCA hens are tumor specific. Two immunoreactive bands (12 & 50kDa) for IL-16 were identified in the ovary while only one band (50 kDa) was detected in sera suggesting that IL-16 may be the active in tetramerized form. IL-16 protein and mRNA expression as well as the frequency of MVD were significantly higher in hens with OVCA than healthy hens. VEGF expressing microvessels were localized in the ovarian stroma preceding the tumor indicating that ovarian TAN precedes tumor progression.
Conclusion: The results of the study suggest that changes in serum levels of IL-16 are positively correlated with tumor initiation and progression. Thus serum IL-16 level together with marker of ovarian TAN may constitute a feasible test for the early detection of OVCA. Support: Prevent Cancer Foundation, Sramak Foundation and DOD (OC#093303).

American Association for Cancer Research
615 Chestnut St. 17th Floor
Philadelphia, PA 19106

Cancer Research: April 15, 2012; Volume 72, Issue 8, Supplement 1
doi: 10.1158/1538-7445.AM2012-3646
Proceedings: AACR 103rd Annual Meeting 2012-- Mar 31-Apr 4, 2012; Chicago, IL

Poster Presentations - Biomarkers of Ovarian, Prostate, and Bladder Cancers

Abstract 3646: Expression of death receptor 6 (DR6) increases in association with ovarian tumor development and progression

Aparna Yellapa[1], Mohammad F. Khan[1], Janice M. Bahr[2], Pincas Bitterman[1], Jacques S. Abramowicz[1], Sanjib Basu[1], Seby L. Edassery[1], and Animesh Barua[1]

[1]Rush University Medical Center, Chicago, IL

[2]University of Illinois at Urbana-Champaign, Urbana, IL

Background: Because of the lack of an early detection test, ovarian cancer (OVCA) remains a lethal malignancy of women. OVCA differs from other malignancies in its specific dissemination pattern that the tumor typically spreads in a diffuse intra-pelvic and abdominal manner. Thus tumor microenvironment plays an important role in tumor dissemination and suppression of anti-tumor immunity is a hallmark of tumor progression. Although the precise mechanism of immune evasion by the tumor is not known, expression of death receptor 6 (DR6) has been suggested to be associated with tumor progression in several malignancies. DR6 is a member of the TNF receptor superfamily and a regulator of immune function. Expression of DR6 by ovarian tumors is unknown. Access to patients at early stage OVCA is very difficult. Laying hens develop OVCA spontaneously with histopathology similar to humans. Objectives: The goal of the present study was to determine whether DR6 is expressed by ovarian tumors at early stage and to examine whether DR6 expression is associated with OVCA tumor progression in the laying hen model of human OVCA. Materials and Methods: 3 years old normal, low or stopped egg-laying hens were scanned by ultrasound, sera were collected, hens were euthanized and ovarian tissues were processed for paraffin and frozen sections, immunoblotting and mRNA extraction. Stages of OVCA were confirmed at gross morphology and routine histology. Samples were divided into 3 groups: normal (control), early and late stages of OVCA. Sera were tested for DR6 levels by ELISA and confirmed by 2D-Western blot (WB). Expression of DR6 by normal and tumor ovaries was examined by immunohistochemistry (IHC), WB and RT-PCR. Results: DR6 was expressed by the epithelium of the ovarian tumor and angiogenic microvessels in the tumor stroma. The population of DR6+ microvessels and serum levels of DR6 was significantly higher in hens with ovarian tumors than the normal hens. Immunoblotting and gene expression analysis confirmed IHC observations. There was a significant increase in DR6 expression in hens with early stage OVCA (including microscopic tumor) suggesting that serum DR6 may be a potential indicator of ovarian tumors at very early stage. The frequencies of DR6+ cells were significantly higher in hens with late stage OVCA than early stage suggesting that DR6 may be involved in ovarian tumor development and progression in laying hens. Conclusion: For the first time, this study showed that epithelial cells in ovarian tumors express DR6 and results suggest that changes in serum levels as well as tissue expression of DR6 are associated with tumor initiation and progression. Thus serum DR6 may be useful as a surrogate maker of OVCA, target for anti-tumor immunotherapy as well as molecular imaging. This study will provide a foundation for a clinical study. Support: DOD (OC#093303), NCI-POCRC (P50 CA83636) and the Elmer Sylvia and Sramek Foundation.

Citation Format: {Authors}. {Abstract title} [abstract]. In: Proceedings of the 103rd Annual Meeting of the American Association for Cancer Research; 2012 Mar 31-Apr 4; Chicago,

Cancer Research: April 15, 2012; Volume 72, Issue 8, Supplement 1
doi: 10.1158/1538-7445.AM2012-5415
Proceedings: AACR 103rd Annual Meeting 2012-- Mar 31-Apr 4, 2012; Chicago, IL

Poster Presentations - Tumor Immunobiology 3

Abstract 5415: Expression of immunosuppressive leukocyte inhibitory immunoglobulin like transcript 3 (ILT3) receptors increases with the development and progression of ovarian tumors

Mohammad F. Khan[1], Aparna Yellapa[1], Janice Bahr[2], Pincas Bitterman[1], Jacques Abramowicz[1], Sanjib Basu[1], Seby Edassery[1], and Animesh Barua[1]

[1]Rush University Medical Center, Chicago, IL

[2]University of Illinois at Urbana-Champaign, Urbana, IL

Background: Immunosuppressive tumor microenvironment has been suggested as one of the barriers to anti-tumor immune response in patient with ovarian cancer (OVCA). Leukocyte Inhibitory Receptor Immunoglobulin-like Transcript 3 (ILT3) has been proposed as a factor involved in the suppression of immune response in several malignancies. However, the expression and role of ILT3 in the development and progression of ovarian tumors has not yet been studied. Objective: The goal of this study was to examine the expression and association of ILT3 in ovarian tumors in laying hen, a preclinical model of OVCA in humans. Methods: A cohort of mature White Leghorn laying hens with normal or low egg laying rates were evaluated by transvaginal ultrasound scan (15 normal hens and 30 hens with OVCA).All hens were euthanized and serum and ovarian tissues from all hens were collected and processed for immunohistochemistry (IHC), Western blotting (WB) and RT-PCR. Presence of tumors and tumor staging were confirmed by gross morphology and histology. Expression of ILT3 was examined by IHC, WB and RT-PCR. Results: Immune cell like cells in the ovarian stroma as well as epithelium of the normal ovaries and ovarian tumors expressed ILT3. The intensity of ILT3 expression was significantly higher in hens with OVCA than normal hens. Moreover, the intensity of ILT3 expression varied with histological subtypes of ovarian tumors and was significantly higher in serous OVCA than endometrioid OVCA. A band of approximately 55kDa of ILT3 protein was detected in the homogenates of normal ovarian surface epithelium or tumor epithelium as well as whole normal or ovarian tumor extracts. Similar to IHC observations, protein expression was stronger in hens with OVCA than in normal hens. Conclusion: This is the first study to show that immunosuppressive ILT3 is expressed by ovarian tumor epithelium and the intensity of expression increases as the disease progresses. Thus the results are consistent with the hypothesis that ILT3 may be involved in the suppression of anti-tumor immunity in OVCA. The laying hens may be a useful model to understand the OVCA-associated expression of ILT3. This animal model also offers the opportunity to develop and test anti-ILT3 therapy to enhance anti-tumor immunity against OVCA in humans. Support: Department of Defense (OC#93303) and Elmer Sylvia and Sramek Foundation.

Citation Format: {Authors}. {Abstract title} [abstract]. In: Proceedings of the 103rd Annual Meeting of the American Association for Cancer Research; 2012 Mar 31-Apr 4; Chicago, IL. Philadelphia (PA): AACR; Cancer Res 2012;72(8 Suppl):Abstract nr 5415. doi:1538-7445.AM2012-5415

Oral Presentations
May 10, 2012
7pm Main Conference Room

Molecular targeted ultrasound imaging of avb3-integrins expressing microvessels in association with anti-NMP antibodies detects ovarian cancer at early stage
Animesh Barua
Departments of Pharmacology, Pathology and Obstetrics & Gynecology, Rush University, Chicago

Ovarian Cancer Survivors' Experiences of Self-Advocacy: A Focus Group Study
Teresa Hagan
University of Pittsburgh School of Nursing, Pittsburgh,PA

Sex-steroid hormones and epithelial ovarian cancer: a nested case-control study
Annekatrin Lukanova
Division of Cancer Epidemiology, German Cancer Research Center, Heidelberg, Germany

Potential effect of the Risk of Ovarian Cancer Algorithm (ROCA) on the mortality outcome of the Prostate, Lung, Colorectal and Ovarian (PLCO) Trial
Paul Pinsky
Division of Cancer Prevention, NCI

Monoclonal antibody-based immunotherapy of ovarian cancer: targeting of differentiated and cancer initiating cells with the B7-H3-specific mAb 376.96 and sunitinib
Donald Buchsbaum
Department of Radiation Oncology, University of Alabama at Birmingham

Meso-TR3: A Novel TRAIL-Based Targeted Therapeutic in Ovarian Cancer
Gunjal Garg
Division of Gynecologic Oncology, Department of Obstetrics and Gynecology, Washington University School of Medicine, St. Louis

PGE2 in ovarian cancer-associated immune dysfunction
Pawel Kalinski
University of Pittsburgh Cancer Institute, Pittsburgh, PA

A genetically engineered mouse model for high grade serous "ovarian" carcinoma arising in the fallopian tube.
Ruth Perets
Department of Medical Oncology, Center for Molecular Oncologic Pathology, Dana-Farber Cancer Institute, Boston, MA

Molecular targeted ultrasound imaging of $\alpha_v\beta_3$-integrins expressing microvessels in association with anti-NMP antibodiesdetects ovarian cancer at early stage

Background: Changes in nuclear morphology including nuclear matrix proteins (NMPs) followed by tumor associated neoangiogenesis (TAN) are the two earlier events in malignant transformation and progression of ovarian cancer (OVCA). Anti-NMP antibodies are produced in response to NMPs shed during malignant transformation. Expression of avb3-integrins by TAN vessels is one of the features of ovarian TAN. Anti-NMP antibodies and ovarian TAN may represent markers of early stage OVCA. Identification of patients at early stage OVCA is very difficult and laying hens have been shown to develop spontaneous OVCA with histopathology similar to humans. The goal of this study was to examine the feasibility of $\alpha_v\beta_3$-integrin targeted transvaginal ultrasound (TVUS) imaging and anti-NMP antibodies in detecting OVCA at early stage.
Methods: Hens with (n= 50)or without (n= 20) serum anti-NMP antibodies and without any TVUS detectable ovarian abnormality were selected for prospective monitoring by avb3-integrins targeted TVUS at 15 weeks interval up to 45 weeks. Hens were scanned before, during and after injection of targeted microbubbles at each interval. Pre- and post-injection images archived and analyzed off-line. Hens were euthanized at diagnosis for OVCA or at the end of the 45 weeks. Gross diagnosis was recorded at euthanasia. Serum and tissues were processed for histology, immunohistochemistry (SMA and $\alpha_v\beta_3$ integrins) and immunoblotting.
Results: Within 30-45 weeks of monitoring, 7 hens with serum anti-NMP antibodies developed OVCA spontaneously. $\alpha_v\beta_3$-integrins targeted microbubles enhanced the visualization of ovarian tumors remarkably. Targeted microbubbles bounded areas appeared as a ring on the ovarian surfaces of 5 hens on TVUS and suspected for OVCA. Tumors were confirmed in all hens predicted to have OVCA by targeted TVUS at euthanasia. In 4 hens, tumors were limited to the ovaries (early stage) and in one hen the tumor metastasized to abdominal cavity. Targeted TVUS imaging could not detect two hens with microscopic lesions without any solid tumor mass. Thus 7 of 50 hens had OVCA and targeted microbubbles detected approximately 72% (5 of 7 hens). Serum reacted against NMP antigens of various molecular wt from malignant ovaries in immunoblotting. The frequency of TAN vessels (SMA and $\alpha_v\beta_3$-integrins expressing) were significantly higher in OVCA hens than normal hens ($P<0.05$).
Conclusions: Targeted imaging enhanced TVUS detection of early stage OVCA. Anti-NMP antibodies together with targeted imaging may constitute an early detection test for OVCA. The results may form the foundation for a clinical study.
Support: Department of Defense (#09-3303), Sramek Foundation.